Critical exponents by the scaling-field method: The isotropic N-vector model in three dimensions

Kathie E. Newman
Department of Physics, University of Notre Dame, Notre Dame, Indiana 46556

Eberhard K. Riedel
Department of Physics, University of Washington, Seattle, Washington 98195
(Received 9 July 1984)

A numerical technique, termed the scaling-field method, is developed for solving by successive approximation Wilson's exact renormalization-group equation for critical phenomena in three-dimensional spin systems. The approach uses the scaling-field representation of the Wilson equation derived by Riedel, Golner, and Newman. A procedure is proposed for generating in a nonperturbative and unbiased fashion sequences of successively larger truncations to the infinite hierarchy of scaling-field equations. A "principle of balance" is introduced and used to provide a self-consistency criterion. The approach is then applied to the isotropic N-vector model. Truncations to order 13 (10, when $N=1$) scaling-field equations yield the leading critical exponents, ν and η, and several of the correction-to-scaling exponents, Δ_m, to high precision. Results for $N=0$, 1, 2, and 3 are tabulated. For the Ising case ($N=1$), the estimates $\nu=0.626\pm0.009$, $\eta=0.040\pm0.007$, and $\Delta_1\equiv\Delta_{400}=0.54\pm0.05$ are in good agreement with recent high-temperature-series results, though exhibiting larger confidence limits at the present level of approximation. For the first time, estimates are obtained for the second and third correction-to-scaling exponents. For example, for the Ising model the second "even" and first "odd" correction-to-scaling exponents are $\Delta_{422}=1.67\pm0.11$ and $\Delta_{500}=1.5\pm0.3$, respectively. Extensions necessary to improve the accuracy of the calculation are discussed, while applications of the approach to anisotropic N-vector models are described elsewhere. Finally, the scaling-field method is compared with other techniques for the high-precision calculation of critical phenomena in three dimensions, i.e., high-temperature-series, Monte Carlo renormalization-group, and field-theoretic perturbation expansions.

I. INTRODUCTION

The scaling-field method (SFM),[1] which is based on Wilson's exact renormalization-group (RG) equation,[2] has been very successful in the study of crossover phenomena in anisotropic N-vector models.[3,4] In this paper the method is developed into a tool for the high-precision calculation of critical phenomena in three-dimensional spin systems.[5] In fact, the approach offers a powerful alternative to the field-theoretic (FT) expansion techniques.[6,7]

The debate concerning the correct numerical values for critical exponents in three-dimensional systems is continuing and focusing increasingly on the values for the correction-to-scaling exponents. The influence of the latter on the critical behavior is always present[8] but difficult to extract from perturbation expansions or experimental data. Work on the critical exponents of the isotropic N-vector model by FT perturbation expansions has had a major impact.[6,7] Specifically, the FT result for the Ising model of $\gamma\approx1.24$ showed significant disagreement with the previously accepted estimate of $\gamma\approx1.25$ from high-temperature (HT) series. The FT technique involves Feynman-graph computations to high order,[9] and requires sophisticated resummation and extrapolation since the expansion parameter, which is the renormalized coupling constant, is not small in three dimensions. Recently, significant progress has been made in HT-series expansions; new techniques for analyzing[10–15] HT series as well as for generating[11,15,16] longer series have been developed. The present consensus seems to be that the HT-series results overlap the FT estimates, although suggesting a slightly higher value for the first correction-to-scaling exponent $\Delta_1\equiv\Delta_{400}$ and a slightly lower one for γ (or a slightly higher one for η).[14] Also being developed currently is the Monte Carlo (MC) renormalization group for the *three*-dimensional Ising model.[17,18] In yet another approach, the critical behavior of the Ising model is simulated by a specially designed MC array processor.[19] The purpose of the present paper is to present a new momentum-space RG approach, termed the scaling-field method, which is applicable to the high-precision calculation of critical exponents of a large class of isotropic and anisotropic N-vector models.

The SFM satisfies two important criteria for high-precision techniques. First, it is based on an exact equation, which is Wilson's functional RG equation, and, second, it proceeds by generating successive approximations systematically. The convergence of the method must be studied *a posteriori*. Although the Wilson functional RG equation appears not to be solvable by direct attack, it has been transformed into an infinite hierarchy of ordinary nonlinear differential equations, termed scaling-field (SF) equations. For background, see Ref. 1, which hereafter will be referred to as I. The key ingredient for the numerical solution of the Wilson equation by successive approximation is the "principle of balance," which we will introduce below. This principle allowed us to formulate a procedure for generating, nonperturbatively, se-

quences of successively larger truncations to the SF equations.

In this paper the SFM is applied to the isotropic N-vector model and the computation of its critical exponents. Specifically, an approximation is considered within which sequences of balanced truncations of up to $n_{eq} \approx 13$ ($n_{eq}=10$, when $N=1$) SF equations can be found. There is no technical reason that forces one to stop at this approximation. Estimates for the leading critical exponents by the SFM for the cases $N=0$, 1, 2, and 3 are presented in Table V. The confidence limits include estimates of systematic errors, and their assignment is described later. To facilitate comparisons, Table VIII exhibits a summary of current estimates for the Ising ($N=1$) critical exponents by the HT, FT, and MC methods. The SF estimates for the Ising exponents are $\nu=0.626\pm0.009$, $\eta=0.040\pm0.007$, and $\Delta_1 \equiv \Delta_{400}=0.54 \pm 0.05$.[20] These values agree well with the HT-series results, although they are less precise in the present approximation. However, like the latter, they suggest slightly higher values for the exponents η and Δ_1 than those obtained by the FT method. For the first time we provide good estimates for the lower-lying correction-to-scaling exponents. For example, for the Ising model, we estimate the second "even" and first "odd" correction-to-scaling exponents to be $\Delta_{422}=1.05\pm0.08$ and $\Delta_{500}=1.5 \pm 0.3$, respectively.[20] These results, which can be approximated by $\Delta_{422} \approx 2\Delta_{400}$ and $\Delta_{500} \approx 3\Delta_{400}$, are of interest in the analysis of experimental data and HT series.[16] Further comparisons are provided in Secs. III and IV.

The SFM differs in several important ways from other techniques.

(i) The approach is nonperturbative. Neither the Wilson equation nor the procedure for generating successively larger truncations involve perturbation-expansion arguments. The implicit assumption in the SFM is that high-precision calculations of critical exponents are possible, based on the expansion of the RG Landau Hamiltonian in terms of Gaussian operators [see Eq. (2.4) below], even if one retains only certain kinds and limited numbers of operators. The nonperturbative character of the SFM makes it possible to compute critical exponents by a simple matrix diagonalization, i.e., without the need for extrapolation or resummation procedures. This yields both the leading and the correction-to-scaling exponents.

(ii) The SFM is applicable with only minor changes to isotropic and anisotropic N-vector models. The reason for this is that the Wilson RG equation holds for general N-component-spin Landau Hamiltonians. As yet, only estimates for the critical exponents of certain classes of anisotropic spin models in three dimensions have been obtained, specifically, for the randomly dilute Ising and cubic N-vector,[3] and the percolation and Q-state Potts problems.[4]

(iii) The SFM allows the investigation of trends in critical phenomena as function of the spatial dimension d (e.g., between the upper and lower critical dimensions) or the number of spin components N.[3,4] This fact has also been used to test the computational algorithm in well-understood limits, such as ϵ expansion or special values of N. Numerical calculations are always performed at the spatial dimension of interest.

(iv) The calculations by the SFM can be easily extended. This applies to the high-precision work for the isotropic N-vector model considered here and our studies for anisotropic systems.[3,4] The steps necessary to calculate additional SF coupling coefficients are described in I. Although the computation involves more complicated combinatorics, which can be performed with the help of algebraic-manipulation programs, the integrals can still be reduced to one-dimensional ones by Fourier-transform techniques. In contrast, extending the HT or FT perturbation expansions poses considerable difficulties, e.g., the evaluation of high-dimensional integrals in the FT approach.[16] For remarks concerning the computation of scaling functions by the SFM, see I.

In summary, it is concluded that the SFM warrants a large-scale computing effort which would yield, to good precision, the leading and correction-to-scaling exponents and other quantities for a variety of three-dimensional N-component-spin systems. In view of the modest length of the truncations considered for the isotropic N-vector model so far, the precision of the results is excellent. The procedure is nonperturbative and yields unbiased results. We believe that the SFM has the potential for overtaking the expansion techniques as the best source of calculated information for three-dimensional N-vector models.

The outline of this article is as follows. In Sec. II we develop the SFM for solving the Wilson RG equation by successive approximation. A procedure is proposed for generating sequences of successively longer truncations to the SF equations that is "blind-folded" to the convergence of the method. In Sec. III we apply the approach to the high-precision calculation of the critical exponents of the isotropic N-vector model. The computation of the correction-to-scaling exponents is dealt with in a special subsection, Sec. III B. In Sec. IV we contrast the SFM with three other techniques for high-precision calculations of critical exponents, i.e., HT-series, MC renormalization-group, and FT perturbation expansions, and compare, at a nontechnical level, the kinds of approximations involved.

II. SCALING-FIELD METHOD

In this section a method of successive approximation for solving the exact Wilson RG equation for critical phenomena of three-dimensional systems is proposed. A "principle of balance" is introduced and used to generate sequences of successively larger truncations. The procedure described has as its principal virtue the fact that it neither biases the results nor prejudices the convergence of the method.

A. Scaling-field equations

The Wilson functional RG equation for RG Hamiltonians of the Landau type, written schematically,[1]

$$\frac{dH_l[\sigma]}{dl} = \mathcal{G}\{H_l[\sigma];\Delta\} , \tag{2.1}$$

is exact and explicit, but no general techniques exist presently for its direct solution. The right-hand side of this evolution equation for $H_l[\sigma]$ as a function of the RG iteration parameter l depends only on $H_l[\sigma]$ and a spin-rescaling parameter Δ (in the notation of Wilson and Kogut,[2] $\Delta=1-d\rho/dl$). Our approach starts from the SF representation of the Wilson equation, which is given in Eq. (2.5) below, and has been derived in I.

We adopt the following notation.[1] The Landau Hamiltonian for the isotropic N-vector model is

$$H_l[\sigma]=\sum_{\bar{m}\ \text{even}}\int_{\underline{q}_1,\ldots,\underline{q}_{\bar{m}}} u_{\bar{m}}(\underline{q}_1,\ldots,\underline{q}_{\bar{m}};l)\delta(\underline{q}_1+\cdots+\underline{q}_{\bar{m}})[\vec{\sigma}(q_1)\cdot\vec{\sigma}(q_2)]\cdots[\vec{\sigma}(q_{\bar{m}-1})\cdot\vec{\sigma}(q_{\bar{m}})]\ . \tag{2.2}$$

In Wilson's formulation, integrals $\int_q \equiv \int d^dq$, extend over all space, and a smooth cutoff function $\psi(q)$ [see Eq. (2.16) below] is absorbed into the definition of the functions $u_{\bar{m}}\{\underline{q}_i;l\}$. The functional variables $\vec{\sigma}(q)$ are N-component "spins"

$$\vec{\sigma}(q)=\{\sigma_\alpha(q);\alpha=1,\ldots,N;-\infty\le\sigma_\alpha(q)\le\infty\}\ .$$

We consider only Hamiltonians that are isotropic both in the spin and momentum variables. The Boltzmann factor $\beta=1/k_BT$ is absorbed in the definition of (2.2) in the usual way. The free-energy density divided by k_BT is given by

$$F\{H_{l=0}\}=-V^{-1}\ln\left\{\int_{[\sigma]}\exp(-H_{l=0}[\sigma])\right\}\ . \tag{2.3}$$

For further definitions, see Appendix A of I. Invoking the universality hypothesis, one refers to the model (2.2) as the Ising, planar, Heisenberg, or spherical model when $N=1$, 2, 3, and ∞, respectively. The case $N=0$ is relevant to the excluded-volume problem and $N=-2$ is the limit of Gaussian critical behavior.

In the SF approach, the RG equations are parametrized by the values of the nonlinear scaling fields $\mu_m(l)$.[1,21,22] One expands $H_l[\sigma]$ about the Gaussian fixed point $H_G^*[\sigma]$, in terms of the set of Gaussian operators $Q_m[\sigma]$,

$$H_l[\sigma]=H_G^*[\sigma]+\sum_m \mu_m(l)Q_m[\sigma]\ . \tag{2.4}$$

[Equations (2.4) and (2.2) are related in Appendix A.] An exact transformation of the Wilson equation (2.1) then leads to the infinite hierarchy of ordinary nonlinear differential equations for the scaling fields $\mu_m(l)$,

$$\frac{d\mu_m(l)}{dl}=y_m^G\mu_m(l)+\sum_{j,k}a_{mjk}\mu_j(l)\mu_k(l)+\sum_j a_{mj}\mu_j(l)+a_m\ , \tag{2.5}$$

termed SF equations. This SF representation is the starting point of our method of successive approximation for solving the Wilson equation. In Eq. (2.5), the y_m^G denote the eigenvalues associated with the Gaussian operators and the a_{mjk},a_{mj},a_m are the SF coupling coefficients, whose computation is discussed in I. Via the coupling coefficients, the SF equations (2.5) depend on the physical characteristics of the system, spatial dimensionality d, number of spin components N, and spin-rescaling parameter Δ, as well as conventions used in the formulation of the Wilson equation. The coupling coefficients depend linearly on Δ,

$$a_{mjk}=a'_{mjk}+\Delta a''_{mjk}\ , \tag{2.6a}$$

$$a_{mj}=\Delta a''_{mj}\ , \tag{2.6b}$$

$$a_m=\Delta a''_m\ . \tag{2.6c}$$

In numerical work, we treat Δ as an input parameter whose fixed-point value Δ^* we determine by a side condition discussed in Sec. II B. The linearization of Eq. (2.5) about a fixed point, $d\mu_m^*/dl=0$ for all m, defines the stability matrix $Y(m,j)$. Using $\delta\mu_m=\mu_m-\mu_m^*$, one obtains, from Eq. (2.5),

$$\frac{d(\delta\mu_m)}{dl}=\sum_j Y(m,j)\delta\mu_j\ , \tag{2.7}$$

with

$$Y(m,j)=y_m^G\delta_{m,j}+2\sum_k a^*_{mjk}\mu_k^*+a^*_{mj}\ , \tag{2.8}$$

where $a^*_{mjk}=a_{mjk}(\Delta^*)$, etc., are defined by Eqs. (2.6). The exponents y_m associated with the fixed point are the eigenvalues of the matrix $Y(m,j)$.

In calculations for the isotropic N-vector model, the operators in the expansion (2.4) are generalized Laguerre polynomials, which are characterized by two principal indices, $\bar{m}$ and p, which label the order in the spins $\vec{\sigma}(q)$ and momenta $\underline{q}$, and an index t, which is used to distinguish between different types of momentum dependence of the same order p. We use an index m to denote this set of labels,

$$m=\{\bar{m},p,t\}\ \text{ or }\ m=\{\bar{m},p_m,t_m\}\ . \tag{2.9}$$

For future reference, we list the following other results.[1] The Gaussian fixed-point Hamiltonian of Eq. (2.1) is

$$H^G_{l=0}[\sigma]=\tfrac{1}{2}\int_{\underline{q}} u_G^*(q)\vec{\sigma}(q)\cdot\vec{\sigma}(-q),\quad \Delta_G^*=0 \tag{2.10a}$$

with

$$u_G^*(q)=Aq^2/[Aq^2+\exp(-2q^2)]\ , \tag{2.10b}$$

A being a normalization parameter. The Gaussian eigenvalues and eigenoperators are

$$y^G_{\bar{m}pt}=d-\frac{\bar{m}}{2}(d-2)-p \tag{2.11}$$

and

$$Q_{\bar{m}pt}[\sigma]=\exp[-P]\bar{Q}_{\bar{m}pt}[\sigma]\ , \tag{2.12}$$

where

$$\exp[-P]=\exp\left[-\tfrac{1}{2}\int_{\underline{q}}[u_G^*(q)]^{-1}\frac{\delta}{\delta\vec{\sigma}(q)}\cdot\frac{\delta}{\delta\vec{\sigma}(-q)}\right] \tag{2.13}$$

and

$$\bar{Q}_{\bar{m}pt}[\sigma]=\frac{1}{\bar{m}!}\int_{\underset{\sim}{q}_1,\ldots,\underset{\sim}{q}_{\bar{m}}} f_{\bar{m}pt}(\underset{\sim}{q}_1,\ldots,\underset{\sim}{q}_{\bar{m}})\delta(\underset{\sim}{q}_1+\cdots+\underset{\sim}{q}_{\bar{m}})\prod_{i=1}^{\bar{m}}\psi(q_i)[\vec{\sigma}(q_1)\cdot\vec{\sigma}(q_2)]\cdots[\vec{\sigma}(q_{\bar{m}-1})\cdot\vec{\sigma}(q_{\bar{m}})]\ . \tag{2.14}$$

The functions $f_{\bar{m}pt}\{\underset{\sim}{q}_i\}$, which parametrize the momentum dependence of the Gaussian eigenoperators, are homogeneous functions of order p in the momenta $\underset{\sim}{q}_i$, $i=1,\ldots,\bar{m}$. For example, for $p=0$ and 2,

$$f_{\bar{m}00}\{\underset{\sim}{q}_i\}=1\ , \tag{2.15a}$$

$$f_{\bar{m}21}\{\underset{\sim}{q}_i\}=\frac{1}{\bar{m}}\sum_{i=1}^{\bar{m}}q_i^2\ , \tag{2.15b}$$

$$f_{\bar{m}22}\{\underset{\sim}{q}_i\}\prod_{i=1}^{\bar{m}}[\vec{\sigma}(q_{2i-1})\cdot\vec{\sigma}(q_{2i})]=\frac{1}{\bar{m}}\left[\sum_{i=1}^{\bar{m}/2}(\underset{\sim}{q}_{2i-1}\cdot\underset{\sim}{q}_{2i})\right]\prod_{i=1}^{\bar{m}}[\vec{\sigma}(q_{2i-1})\cdot\vec{\sigma}(q_{2i})]\ . \tag{2.15c}$$

Note that for $N\neq 1$ there are two types of $p=2$ functions ($t=1,2$) when $\bar{m}>2$, but only one when $\bar{m}=2$; the latter is due to the momentum-conserving δ function between $\underset{\sim}{q}_1$ and $\underset{\sim}{q}_2$ in $Q_{221}[\sigma]$. Similarly, for $p=4$ and $\bar{m}=2$, there is only the function $f_{241}(q)=q^4$. When $N=1$, the operators $Q_{\bar{m}21}[\sigma]$ and $Q_{\bar{m}22}[\sigma]$ are linearly dependent. For further details, see Sec. III B and Appendix C of I. Finally, the momentum integrals extend over all space and are effectively cut off by the factors $\psi(q_i)$, where

$$\begin{aligned}\psi(q)&=\exp(-q^2)/[Aq^2+\exp(-2q^2)]\\&=\{u_G^*(q)[1-u_G^*(q)]/Aq^2\}^{1/2}\ .\end{aligned} \tag{2.16}$$

The forms of this auxiliary function and of $u_G^*(q)$ in Eq. (2.10) are the results of conventions used in the formulation of the Wilson RG equation.[2]

In numerical studies, the hierarchy of SF equations (2.5) must be studied in *truncations* of manageable size. (Solutions by asymptotic expansions in ϵ or $1/N$ were obtained in I and Refs. 3 and 4.) This raises the following questions:

(i) The choice of operators to be retained in the truncated expansions (2.4).

(ii) The extraction of physical information (e.g., critical exponents) from truncated sets of SF equations (2.5).

An approach of successive approximation must be based on procedures that exclude (as far as possible) subjective or biased decisions. Question (i) is answered in Sec. II C, where a systematic procedure for generating successively larger truncations is developed. Question (ii), which arises because truncating the hierarchy of SF equations causes some loss of universality, is discussed in Secs. II B and II C 2. The answers to both questions require a self-consistency principle that allows one to decide which truncations are admissible in high-precision work. In Sec. II B, we introduce the "principle of balance" to serve that purpose. One may argue that the choice of truncations that are admitted biases the results. This is not the case. In contrast to earlier work,[21] the "principle of balance" sets into motion a "blind-folded" procedure for generating systematically improvable results.

We label truncations to Eqs. (2.4) or (2.5) by specifying the numbers of operators (or scaling fields) of *each* kind that are retained. The notation

$$\mathrm{Trun}(n_0,n_{21},n_{22},n_{41},\ldots)\ \text{ when } N\neq 1 \tag{2.17}$$

denotes that the truncation includes the *first* n_0 operators $Q_{\bar{m}00}[\sigma]$ (i.e., $\bar{m}=2,4,\ldots,2n_0$), the *first* n_{21} operators $Q_{\bar{m}21}[\sigma]$ (i.e., $\bar{m}=2,4,\ldots,2n_{21}$), etc. However, since $Q_{222}[\sigma]=-Q_{221}[\sigma]$, we always choose $n_{22}=n_{21}-1$. When $N=1$, $Q_{\bar{m}21}[\sigma]$ and $Q_{\bar{m}22}[\sigma]$, as well as other sets of operators, are linearly dependent. Then fewer types of operators occur and the notation

$$\mathrm{Trun}(n_0,n_{21},n_{41},\ldots)\ \text{ when } N=1 \tag{2.18}$$

is used. The total number of equations n_{eq} for a given truncation is

$$n_{\mathrm{eq}}=\sum_{p,t}n_{pt}\ , \tag{2.19}$$

i.e.,

$$n_{\mathrm{eq}}=n_0+n_{21}+n_{22}+n_{41}+\cdots$$

(with $n_{22}=0$ when $N=1$). The parameters shown explicitly in the above definitions suffice to characterize all truncations involving only operators with $p=0$, 2, and 4 ($\bar{m}=2$). Only for those operators have the coupling coefficients a_{mjk} been computed so far.[1]

The calculation of the eigenvalues y_m from truncated sets of SF equations is done by diagonalizing the corresponding truncated $n_{\mathrm{eq}}\times n_{\mathrm{eq}}$ matrix $Y(m,j)$ of Eq. (2.8). We *label* the eigenvalues by the indices of the corresponding scaling fields, i.e., instead of the usual notation $y_T, y_{T2},\ldots$ and $y_H, y_{H2},\ldots$ for the leading thermal and magnetic eigenvalues, we use $y_{200}, y_{400},\ldots$ and $y_{100}, y_{300},\ldots$, respectively. Our notation is necessary for identifying the lower-lying irrelevant eigenvalues, such as y_{421}, y_{422}, and y_{241}, etc., since these may cross as a function of N or d (e.g., see Figs. 11 and 12 below). We are able to label unambiguously the eigenvalues by considering first short truncations, for which the identification is trivial, and then observing which new eigenvalue or eigenvalues enter when the length of the truncation is increased. Any ambiguity in notation can be resolved by following the eigenvalue, as function of N, to either $N=\infty$ or $N=-2$. The notation $y_{\bar{m}pt}$ does *not* imply that the eigenvector associated with this eigenvalue has as its dominant component the field $\mu^*_{\bar{m}pt}$. For the critical fixed point in three dimensions, this is generally not the case. The calculations for $N=1$ can be performed with

the basis appropriate for $N \neq 1$. The spurious eigenvectors are clearly identifiable since they have vanishing components in the directions indexed by $\overline{m}00$.[1] The critical exponent ν and the correction-to-scaling exponents Δ_m follow from the usual relations, e.g.,

$$\nu = 1/y_{200}, \quad \Delta_{400} = -y_{400}/y_{200}, \quad \Delta_m = -y_m/y_{200} . \tag{2.20}$$

The correlation-function exponent η can be computed from[1]

$$\eta = 2\Delta^* , \tag{2.21}$$

or it can be obtained from the result for the leading magnetic exponent $y_H \equiv y_{100}$, via

$$y_{100} = \tfrac{1}{2}(d+2-\eta) . \tag{2.22}$$

For the case of the Ising model $N=1$, we have tested the consistency of these two methods as discussed in Sec. III B *3*.

B. Analysis of truncated sets of SF equations

To characterize the different behaviors encountered in the study of truncated SF equations, we introduce the following terminology:

(i) The concept of *balance* evolved empirically during our studies and different aspects of it will be elucidated here and in the following sections. Most crudely, fixed points do not exist unless, in the truncated expansion (2.4), the different and competing operators $Q_m[\sigma]$ are represented in a certain "balanced" way. This is easily understood for anisotropic N-vector models, where operators of isotropic and anisotropic symmetry in the spin variable $\vec{\sigma}(q)$ compete. For example, in studies of cubic and Potts models,[3,4] we used truncations that retained in Eq. (2.4) all isotropic *and* anisotropic operators to order σ^6 with $p=0$ and the marginal redundant operator $Q_{221}[\sigma]$. For high-precision calculations the situation is more subtle. Then one must also carefully balance the competing contributions of operators $Q_{\overline{m}pt}[\sigma]$ with different dependences on the momentum and the spin. (We restrict the discussion again to the isotropic N-vector model.) For example, in a calculation that employs only the operators $Q_{\overline{m}pt}[\sigma]$ of order $p=0$ and 2 in the momentum, but of arbitrary order $\overline{m} \geq 2$ in the spin, we find that the largest possible "balanced" truncations contain only 12 SF equations (or 10 SF equations for the Ising case, $N=1$). Furthermore, if we attempt to improve that calculation by including $p=0$ or 2 operators with larger $\overline{m}$, we find that, instead, the truncations exhibit increasingly irregular behavior until finally the fixed point is lost. One might expect this result already from a ranking of the relative importance of the operators $Q_{\overline{m}pt}[\sigma]$ in Eq. (2.4) by the values of the Gaussian eigenvalues (2.11).

(ii) The term *balanced truncation* is used to denote truncations that exhibit fixed-point behavior that is closely analogous to that of the untruncated RG equations (e.g., the Gaussian fixed-point solution, or ϵ expansion). There will always be some loss of universality when the device of truncation is used. Our criterion for "normal" or "balanced" behavior is multifaceted: Fixed points exist but exhibit a typical "false" fixed-line behavior as function of Δ (to be described below); the spectrum of eigenvalues contains few complex pairs among the correction-to-scaling eigenvalues (see Sec. III A *2*); and the potential associated with the fixed-point Hamiltonian is thermodynamically stable in all or most of its coordinates (see Sec. II C *3*). Large truncations become increasingly sensitive to proper balancing, which is consistent with the fact that universal behavior is approached (compare Sec. II C *4*).

(iii) Truncations that exhibit no fixed point or show abnormal fixed-point behaviors are called *aberrant* or *unbalanced*. There are some borderline cases of "almost balanced" truncations.

(iv) In Sec. II C, a procedure for generating *sequences* of successively larger balanced truncations is introduced. Only the balanced truncations that appear in these sequences are admitted to the data analysis. The procedure uses a *marker* scaling field to signal the end of sequences of balanced truncations and to optimize the calculation by maximizing the length of such sequences.

(v) The above ideas are summarized by the term *principle of balance*. The principle of balance provides the self-consistency criterion for the generation of sequences of successive truncations in our approach for solving the Wilson equation. For operational definitions of the above concepts, see the "rules for generating sequences" at the end of Sec. II C *1*.

In the remainder of this section we consider typical balanced truncations, emphasizing the determination of the fixed-point value Δ^* of the spin-rescaling parameter Δ. The significance of Δ^* lies in the fact that this parameter is directly related to the value of the correlation-function exponent η, via Eq. (2.21), and indirectly to all other critical exponents, via Eq. (2.8). In numerical work, Δ is treated as an input parameter. For the untruncated equations one expects fixed points to exist for discrete values of the spin-rescaling parameter Δ, which we label Δ_e^*, the subindex denoting "exact." A similar situation exists for asymptotic expansions, i.e., ϵ or $1/N$ expansions, where Δ_e^* can be determined analytically under certain conditions. (For details, see Sec. V of I.) The fixed-point value Δ_e^* is universal for a manifold of equivalent fixed-point Hamiltonians $H_\zeta^*[\sigma]$ that are those that differ only by the values of redundant parameters, ζ.[23,24] In I this was shown specifically for the transformation U_ζ that changes the scales of the spin and momentum variables by ζ:

$$\vec{\sigma} \to \vec{\sigma}/\zeta \quad \text{and} \quad q^2 \to \zeta q^2 . \tag{2.23}$$

The operator $\mathscr{G}_1\{H_\zeta^*[\sigma]\}$ that generates motion in the redundant direction [see Eqs. (2.36) and (2.37) of I] is marginal, i.e., it has zero eigenvalue.

When truncations are considered, the situation is different. The truncated form of this operator, $\mathscr{G}_1'\{H_\zeta^*[\sigma]\}$ (indicated by a prime), is no longer necessarily redundant and marginal, i.e., universality is violated. This is seen in two interconnected ways: Exponents and other universal quantities show nonuniversal behavior as function of ζ and fixed points exist for a continuous *range* of Δ rather than a discrete value of Δ_e^* only. We resolve the latter ambiguity by observing that, for a certain value of Δ, a marginal operator $Q_\kappa'[\sigma]$ can still be found (with

$Q'_\kappa[\sigma] \sim \mathscr{G}'_1\{H^*_\zeta[\sigma]\}$), and we use this vestige of the exact RG equation as a side condition to determine the best approximation Δ^* to the unknown Δ^*_e. Our side condition, which is stated in Eq. (2.27) below, is similar to an idea proposed by Bell and Wilson.[25] The ambiguity of the ζ dependence is resolved by choosing the scale of the spin and momentum variables such that the effect of the operators $Q_{\bar{m}pt}[\sigma]$ missing from the truncation is minimized. This is discussed in detail in Sec. II C 2. Such a determination is not unlike the "gauge" choice used in our ϵ-expansion work, which there had the purpose of making possible the analytical solution of the equations. Since the SF expansion (2.4) is about the Gaussian fixed point, we select the Gaussian normalization A in Eq. (2.10b) as our "model" redundant parameter.

In I we showed that, for the Gaussian fixed point (2.10), the parameter A is related to the choice of normalization of spin and momentum [Eq. (3.8) of that reference]. The redundant direction generated by varying A is associated with the operator $Q_{221}[\sigma]$ with marginal eigenvalue $y^G_{221}=0$ [see Eqs. (2.11) and (2.14)], i.e.,

$$\frac{\partial H^*_G}{\partial A} = Q_{221}[\sigma] = (2A)^{-1}\mathscr{G}_1\{H^*_G[\sigma]\} \tag{2.24}$$

[see Eq. (5.3) of I]. This means that the line of Gaussian fixed points can be parametrized either by A *or* by the fixed-point coordinate μ^*_{221}. This can also be seen directly from Eq. (2.10b). Replacing A by $A'=A+\delta A$, one obtains

$$u^*_G(q;A') = u^*_G(q;A) + \psi^2(q;A)[(\delta A)q^2 - (\delta A)^2 q^4 + \cdots], \tag{2.25}$$

i.e., the fixed point at A' with $\mu^*_{2p\,1}=0$, for all p, is equivalent to the one at A with $\mu^*_{221}=\delta A$, $\mu^*_{241}=-(\delta A)^2$, etc., which shows that all operators $Q_{2p\,1}[\sigma]$, with $p\geq 2$, are redundant at the Gaussian fixed point.[1] Hence the line of Gaussian fixed points parametrized by μ^*_{221} has the following properties:

$$\text{(i)}\quad \mu^*_{241} = -(\mu^*_{221})^2, \ldots, \tag{2.26a}$$

$$\text{(ii)}\quad \Delta^*_G = 0 \text{ for all } \mu^*_{221}, \tag{2.26b}$$

and

$$\text{(iii)}\quad y^G_{221}(\Delta^*_G) = 0 \text{ for all } \mu^*_{221}. \tag{2.26c}$$

For further comments, see Appendix B, where the limit $N=-2$ is discussed, or see Sec. V of I, where the use of the gauge choice $\mu^*_{221}=0$ for the solution by ϵ expansion is discussed.

Remnants of the above behavior are found for the critical fixed points exhibited by balanced truncations. Figures 1(a)–1(c) show such results for a typical balanced truncation, Trun(4,4,1) with $A=3$, for the three-dimensional Ising model ($N=1$). We make the following observations [using the same subheadings as in Eqs. (2.26)]:

(i) Truncating the SF equations leads to "false" fixed-line behavior as a function of Δ. Now view this behavior as being parametrized in terms of the fixed-point coordinate $\mu^*_{221}=\mu^*_{221}(\Delta)$. The parabolic shape of $\mu^*_{241}(\Delta)$ versus

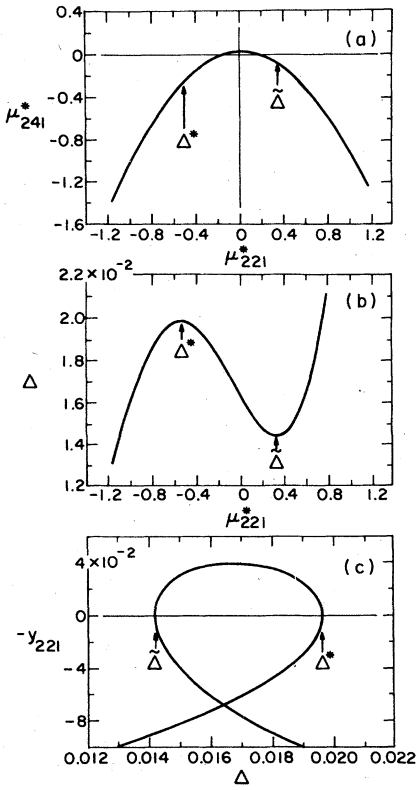

FIG. 1. Remnants of fixed-line behavior exhibited by truncated SF equations: (a) SF coordinates $\mu^*_{241}(\Delta)$ versus $\mu^*_{221}(\Delta)$; (b) spin-rescaling parameter Δ versus SF coordinate $\mu^*_{221}(\Delta)$; (c) negative of the almost-marginal eigenvalue, $-y_{221}(\Delta)$, versus the spin-rescaling parameter Δ. The locations of $y_{221}(\Delta)=0$ are marked by Δ^* and $\tilde{\Delta}$. Data is for $N=1$ from the truncation Trun(4,4,1) with $A=3$.

$\mu^*_{221}(\Delta)$ shown in Fig. 1(a) is reminiscent of the result (2.26a) for the line of Gaussian fixed points. The result is found for small values of the fixed-point coordinates, for which the SF expansion applies.

(ii) The "variation" of the parameter Δ with $\mu^*_{221}(\Delta)$ is shown in Fig. 1(b). We interpret the striking "S" shape of this curve as showing the attempt by the truncation to confine Δ to the fixed-point value. Fixed-point coordinates are typically single- or triple-valued functions of Δ.

(iii) For an exact fixed line, with $\Delta^*=\Delta^*_e$, the operator associated with the redundant direction has zero eigenvalue $y_{221}=0$. For balanced truncations, one typically finds a "loop" for $-y_{221}$ as a function of Δ, as shown in Fig. 1(c). Two locations, denoted Δ^* and $\tilde{\Delta}$, are special, in that for those values $y_{221}(\Delta)=0$. In the interval $\mu^*_{221}(\Delta^*)\leq\mu^*_{221}(\Delta)\leq\mu^*_{221}(\tilde{\Delta})$, the eigenvalue $y_{221}(\Delta)\leq 0$, and, therefore, the corresponding singly unstable fixed points are accessible from the physical subspace $H_{l=0}[\sigma]$ by adjusting one temperaturelike parameter (which is μ_{200} to leading order). The locations Δ^* and $\tilde{\Delta}$ match with the points in Fig. 1(b), where $d\Delta/d\mu^*_{221}=0$, i.e., the regions where the fixed points are (locally) confined to a plane of constant Δ, $\Delta^*=$const (or $\tilde{\Delta}=$const). These two features together single out the values Δ^* and $\tilde{\Delta}$.

Studying balanced truncations in exactly solvable limits suggests that one should select Δ^* to define uniquely the critical fixed point. Therefore, we determine Δ^* by searching for the largest value of Δ that produces a critical fixed point with marginal eigenvalue,

$$y_{221}(\Delta^*)=0 . \tag{2.27}$$

We give the following reasons for this side condition.

(i) Short truncations. Short truncations always exhibit a positive Δ^* even if no "loops" [as seen in Fig. 1(c)] are found (as for truncations with $n_{21}=1$), or if large "loops" with negative $\tilde{\Delta}$ are found [as for Trun(3,2,1,0)].

(ii) Numerical ϵ expansion. One can study the effect of criterion (2.27) close to four dimensions, e.g., for $d=3.99$ by numerical ϵ expansion.[3] (Compare also Sec. V A of I.) For truncation Trun(2,1,0,0), which is sufficient for ϵ-expansion work to leading order, one finds a critical fixed point as function of Δ with $\mu^*_{200}\sim O(\epsilon^2)$, $\mu^*_{400}\sim O(\epsilon)$, and $\mu^*_{221}\sim O(\epsilon^2)$. The η determined from Δ^* agrees with the analytic result

$$\eta=(N+2)\epsilon^2/[2(N+8)^2]+O(\epsilon^3) .$$

(iii) Limit $N=-2+\delta$, δ small. For $N=-2$, the SFM reproduces exactly the Gaussian exponents and line of fixed points. Details are given in Appendix B. The "false" fixed-line behavior is exhibited in Fig. 2 by graphs of $-y_{221}(\Delta)$ versus Δ and $-y_{221}(\Delta)$ versus $\mu^*_{221}(\Delta)$, respectively, obtained from Trun(3,2,1,0) with $A=2$ for a sequence of N approaching -2. No fixed-point solution exists for $\Delta\gtrsim\Delta^*$. The location of Δ^*, the width of the loops, and the maximum amplitude of the loops scale linearly with $\delta=N+2$. Figure 2(b) shows that for $\Delta\approx\Delta^*$ (but not for $\Delta\approx\tilde{\Delta}$) the solution for the truncation has an almost-marginal eigenvalue over an extended region of μ^*_{221}, as $N\to-2$. Hence we conjecture that Δ^* connects smoothly with the exact result $y_{221}(\Delta^*_e=0)=0$ found at $N=-2$ for all $\mu^*_{221}(\Delta^*_e)$.

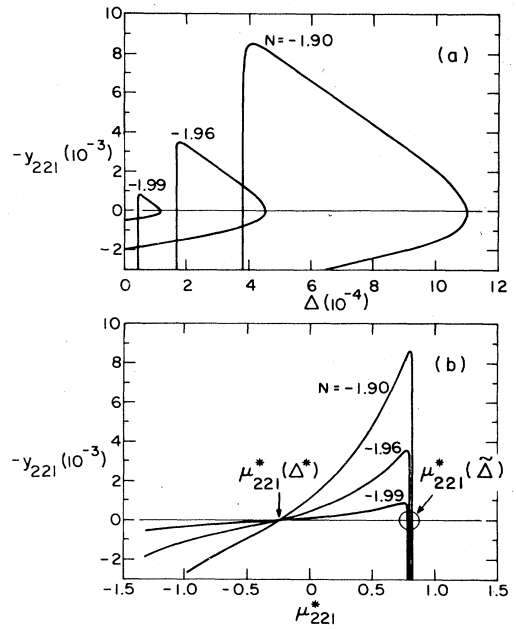

FIG. 2. Remnants of fixed-line behavior in the limit $N=-2+\delta$, $\delta\ll 1$, from the truncation Trun(3,2,1,0) with $A=2$: Negative of the almost-marginal eigenvalue, $-y_{221}(\Delta)$, versus (a) the spin-rescaling parameter Δ and (b) the SF coordinate $\mu^*_{221}(\Delta)$. Exact results are approached for $\delta\to 0$. The right and left locations of $y_{221}(\Delta)=0$ in (a) are referred to as Δ^* and $\tilde{\Delta}$, respectively.

Here we add a comment concerning the linkage of the operator $\mathcal{G}_1\{H^*[\sigma]\}$ with the marginal redundant operator $Q_\kappa[\sigma]$, discussed in Sec. II B of I. This linkage supports our procedure for analyzing truncated sets of SF equations. In the SF representation, $Q'_\kappa[\sigma]$ is given by the eigenvector associated with the marginal eigenvalue $y_{221}(\Delta^*)=0$, which we will denote by $\vec{\iota}$ with components ι_m, while, as shown in Eqs. (2.38) and (2.39) of I, $\mathcal{G}'_1\{H[\sigma]\}$ can be represented as a vector $\vec{\lambda}$ with components λ_m, which, when evaluated at the fixed point $H^*[\sigma]$, is written as $\vec{\lambda}^*$, with

$$\lambda^*_m=a''_m+\sum_j{}' a''_{mj}\mu^*_j+\sum_{j,k}{}' a''_{mjk}\mu^*_j\mu^*_k . \tag{2.28}$$

[The sums marked by primes are over truncated sets of scaling fields, and the coupling coefficients a''_{mjk}, etc., are defined in Eq. (2.6).] Using least-squares analysis to compare the components ι_m with λ^*_m, we define the correlation r,

$$r=\left|\sum_m{}'(\iota_m\lambda^*_m)\right| \Big/ \left[\sum_m{}'(\iota_m)^2\sum_m{}'(\lambda^*_m)^2\right]^{1/2} . \tag{2.29}$$

Typically, we find values of $r\approx 0.95$ for truncations with $n_{eq}=10$ or 11 for the Ising model ($N=1$).

The above discussion has been for a constant value of our "model" redundant parameter A. The viewpoint, that the variation of Δ maps out a portion of a genuine fixed line, proved useful in determining the best numerical value, Δ^*, at which critical exponents should be calculated. Thus, the first seemingly ambiguous aspect of the SF calculation of critical exponents is removed and turned to advantage. We will apply a variation of this argument in Sec. II C 2, where we show that for different values of A, different portions of that fixed line are generated. We will argue that A can be chosen so as to minimize the need for operators $Q_{\bar{m}pt}[\sigma]$ in the SF expansion (2.4) that are presently inaccessible because the corresponding SF coupling coefficients a_{mjk} have not yet been determined. This then turns the second seemingly ambiguous aspect of the SF calculation into a benefit.

C. Generating successive approximations

1. *Sequences of truncations*

An approach of successive approximation must be based on procedures that exclude (as far as possible) subjective or biased decisions. Here we address the technical question of how to generate sequences of truncations of increasing length without biasing the results or prejudicing the convergence of the method.

In generating sequences of truncations, we distinguished between "static" and "dynamic" procedures,

and discarded as ineffective all static procedures. Static procedures are those that first rank the importance of scaling fields μ_m in Eq. (2.5), or operators $Q_m[\sigma]$ in the expansion (2.4), by their eigenvalues y_m at a fixed point *different* from the one of interest, and then define truncations by retaining the equations for all scaling fields with y_m greater than a certain negative number. For example, we attempted to rank the scaling fields according to their eigenvalues y_m^G at the Gaussian fixed point in three dimensions [see Eq. (2.11)] or by the eigenvalues $y_m^{(\epsilon)}$ at the critical fixed point in $d=4-\epsilon$ dimensions, which were calculated to leading order and then extrapolated to $\epsilon=1$. (For a tabulation of $y_m^{(\epsilon)}$, see Table I of I.) We found that both schemes become unstable for larger truncations, i.e., they either fail to produce fixed points or produce fixed points that behave abnormally as a function of Δ.

In dynamic procedures for generating sequences of truncations, the selection of successively larger truncations is guided by feedback from the fixed point under consideration. Increasing the length of a truncation occurs by including one or more additional terms in the expansion (2.4). In turn, this increases the number $n_{\rm eq}$ of coupled SF equations (2.5) to be considered. For simplicity, we will speak of adding "new" scaling fields $\mu_{\bar{m}pt}$ to some "old" truncation of SF equations. When $p>0$, the group of scaling fields $\mu_{\bar{m}pt}$, with $t=1,2,\ldots,t_p$, is added simultaneously. Two questions must be addressed. First, there is, in general, a choice among several types of scaling fields that can be added. After extensive tests, which will be described below, we have adopted the following procedure. Given a balanced truncation, whose properties are well understood, we generate a sequence of truncations by adding successively the scaling field(s) that cause the largest shift in the results for the critical exponents $1/\nu=y_{200}$ and η. Second, in practice, not all kinds of scaling fields are available for constructing truncations. The most time-consuming part of the SF calculation of critical exponents is the determination of the coupling coefficients a_{mjk},[1] which are typically determined for $p\le p'$ (here, $p'=2$). We thus adopted the following rule to assure self-consistency. We include a "marker" scaling field in the calculation, which we chose to be the simplest field of the inaccessible set, i.e., $\mu_{\bar{m}=2,p'+2,t=1}$, and stop the procedure of generating larger truncations when the marker scaling field is required for the first time.

By understanding the mechanisms that control dynamic procedures for generating balanced truncations, we may answer, at least partially, why we can expect to calculate critical exponents to high precision from SF expansions that retain only certain kinds and limited numbers of scaling fields [or, respectively, operators in the expansion (2.4)]. The importance of a newly added scaling field to a given truncation can be measured in terms of the numbers and strengths of its couplings $a_{mjk}\mu_j\mu_k$, etc. to the "old" SF equations. Consider the matrix $Y(m,j)$ of Eq. (2.8), which characterizes the stability of the RG flow in the vicinity of the critical fixed point $\{\mu_m^*\}$. The structure of this matrix is shown schematically in Fig. 3. The diagonalization of this matrix yields the eigenvalues y_m associated with the fixed point $\{\mu_m^*\}$. For calculations to leading order in ϵ expansion, this matrix is *block diagonal,*

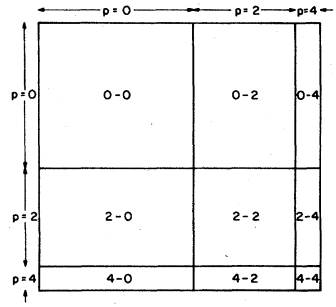

FIG. 3. Schematic representation of the fixed-point matrix $Y(m,j)\equiv Y(\bar{m},p_m,t_m;\bar{j},p_j,t_j)$ of Eq. (2.8) for a truncated set of SF equations. The matrix is arranged in blocks characterized by subindices (p_m,p_j); inside each block (not shown explicitly) the indices m,j are in the order $\{\bar{m},0,0\}$ for $\bar{m}=2,4,\ldots,2n_0$; $\{2,2,1\}$; $\{\bar{m},2,1\}$ and $\{\bar{m},2,2\}$ for $\bar{m}=4,6,\ldots,2n_{21}$, etc.

and the blocks that must be diagonalized couple only scaling fields that differ by the degeneracy index t, i.e.,

$$\bar{Y}_{i,i'}\equiv Y(\bar{m},p,t_i;\bar{m},p,t_{i'})\ ,$$

as shown in Sec. V A of I. A similar simplification is found for calculations in the limit $N\to\infty$. Then the matrix is *triangular,* i.e.,

$$Y(\bar{m},p_m,t_m;\bar{j},p_j,t_j)=0$$

for $\bar{m}<\bar{j}$. (For details, see Sec. V B of I.) However, for dimension $d=3$ and general N, the matrix $Y(m,j)$ has no simple form and must be diagonalized numerically. However, since some coupling coefficients a_{mjk} are zero either due to the linked-contraction condition [defined in Eqs. (4.7) and (4.8) of I] or due to the symmetry of the sets of homogeneous functions $f_{\bar{m}pt}\{q_i\}$ involved (see Appendix D of I), certain general statements can be made about the form of $Y(m,j)$. We order the matrix elements $Y(\bar{m},p_m,t_m;\bar{j},p_j,t_j)$ into blocks p_m-p_j (see Fig. 3). The blocks 0-0, 2-2, 4-4, etc. contain more nonzero and stronger couplings $a^*_{mjk}\mu^*_k$ than blocks 0-2, 0-4, 2-4, etc. Numerically, we find that the matrix elements $Y(\bar{m},p_m,t_m;\bar{j},p_j,t_j)$ of these off-diagonal blocks decrease typically by 1 order of magnitude for each step increase in $\bar{j}$. We conclude that when computing the leading eigenvalue of block 0-0 to high precision, i.e., $y_{200}=1/\nu$, the form of the coupling coefficients a_{mjk} suggests that the scaling fields μ_m with $m=\{\bar{m},0,0\}$ are required in Eq. (2.5) before those with $\{\bar{m},2,t\}$, which, in turn, are required before those with $\{\bar{m},4,t\}$, etc. Fortunately, in practice, one does not have to keep track of the specific form of $Y(m,j)$ (and the couplings $a^*_{mjk}\mu^*_k$), but rather can measure the need for a given new scaling field by its effect on the calculated critical exponents. The remainder of this subsection describes such a procedure.

The test case of the dynamic procedure for generating sequences of balanced truncations was the three-dimensional Ising model ($N=1$). The approximation used retained only the scaling fields $\mu_{\bar{m}pt}$ with $p\le p'=2$ and the "marker" μ_{241}. Starting from the short trunca-

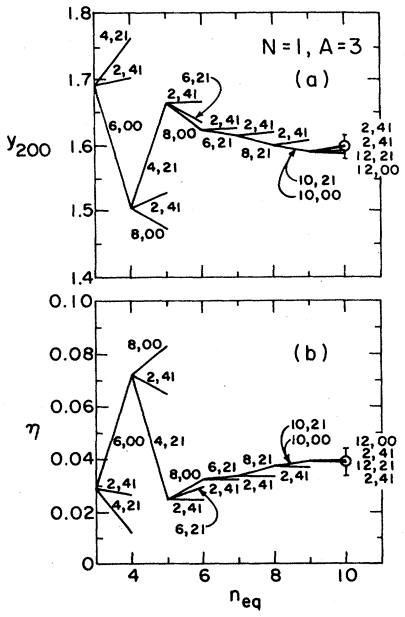

FIG. 4. (a) Thermal exponent y_{200} and (b) correlation-function exponent η of the Ising model versus the number n_{eq} of SF equations for truncations with $A=3$. The labels $\{\bar{m},p,t\}$ denote the scaling field added to the preceding balanced truncation. The continuous line traces the exponent values of the sequence of balanced truncations. The determination of error bars is discussed in Sec. III A.

tion Trun(2,1,0), the procedure generated, without difficulties, balanced truncations that show normal (in the sense of Sec. II B) fixed-point behaviors. Figures 4(a) and 4(b) exhibit the thermal eigenvalue $y_{200}=1/\nu$ and the correlation-length exponent $\eta=2\Delta^*$ as functions of the length of the truncation for $3\leq n_{eq}\leq 10$ with the choice of the normalization parameter $A=3$. The label on the lines in this figure indicate the indices $m=\{\bar{m},p,t\}$ of the scaling field last added to Eq. (2.5). The *sequence of balanced truncations* is defined by those successive truncations that exhibit the largest change in y_{200}, relative to the value obtained from the preceding balanced truncation. When the shifts in y_{200} are almost equal and, therefore, inconclusive for the identification of the next balanced truncation, the shifts in η are used to identify the next new truncation. In general, the largest shifts in y_{200} and η are correlated. In a few cases (e.g., $n_{eq}=10$ in the present sequence), neither the shifts in y_{200} nor those in η allowed us to discriminate between possible scaling fields to be added; then, both truncations were accepted as new balanced truncations. The sequences of balanced truncations are A dependent and are tabulated in Table I for $A=1$, 2, 3, and 4. We note that the largest balanced truncations at the present level of approximation are found with $A=2$ and 3 and have $n_{eq}=10$. (A dependence is further discussed in the following subsection.) The largest balanced truncation in each sequence is the one that includes the marker μ_{241} for the first time. This criterion for terminating the sequence of truncations works by determining when this scaling field becomes *as important* to the calculation of critical exponents as the scaling fields $\mu_{\bar{m}pt}$ with $p\leq p'=2$. Larger truncations can be found, but their fixed points show increasingly abnormal behaviors until the considered fixed points disappear. We view this as an indication of the soundness of our self-consistency procedure based on the principle of balance (see Sec. II B), and do not admit into our data analysis any truncations with larger n_{eq} than shown in Table I. The advantage of our procedure for generating sequences of truncations is that it can be performed without prejudice. Simply, the need for a "new" scaling field μ_m in the larger truncation is measured by the effects it has on the values of the critical exponents. As the results in Fig. 4 indicate, large oscillations in the values of the exponents occur for short truncations and then damp out as n_{eq} is increased. The assignment of error bars, as determined from these types of figures, is discussed in Sec. III A.

In summary, sequences of balanced truncations to the SF equations (2.5) are determined by the following rules. For simplicity, the wording of these rules applies to the approximation considered in this article (i.e., truncations that retain the scaling field $\mu_{\bar{m}pt}$ with $p=0$, $t=0$ and $p=2$, $t=1$ and 2, for arbitrary $\bar{m}\geq 2$, as well as μ_{241}). Their generalization is straightforward (see also Sec. II C *4*).

(1) Begin with a short truncation for which y_{200}, y_{400}, and η can be computed, e.g., Trun(2,1,0,0).

(2) Add one or two "new" scaling fields to the "old"

TABLE I. Sequences of truncations for the Ising model, generated by the procedure described in Sec. II C *1*, for four values of the redundant parameter A. The balanced truncations are underlined. The total number of equations in each truncation is denoted by n_{eq}; see Eq. (2.19). Two balanced truncations exist for $A=3$, when $n_{eq}=9$ and 10.

n_{eq}	$A=1$			$A=2$				$A=3$			$A=4$	
3		2,1,0			2,1,0			2,1,0			2,1,0	
4	3,1,0	2,2,0	2,1,1	3,1,0	2,2,0	2,1,1	3,1,0	2,2,0	2,1,1	3,1,0	2,2,0	2,1,1
5	4,1,0	3,2,0	3,1,1	4,1,0	3,2,0	3,1,1	4,1,0	3,2,0	3,1,1	4,1,0	3,2,0	3,1,1
6	4,2,0	3,3,0	3,2,1	4,2,0	3,3,0	3,2,1	4,2,0	3,3,0	3,2,1	4,2,0	3,3,0	3,2,1
7	4,3,0	3,4,0	3,3,1		4,3,0	4,2,1		4,3,0	4,2,1		4,3,0	4,2,1
8					4,4,0	4,3,1		4,4,0	4,3,1			
9				5,4,0	4,5,0	4,4,1	5,4,0	4,5,0	4,4,1			
10						4,5,1	6,4,0	4,6,0	5,4,1 4,5,1			

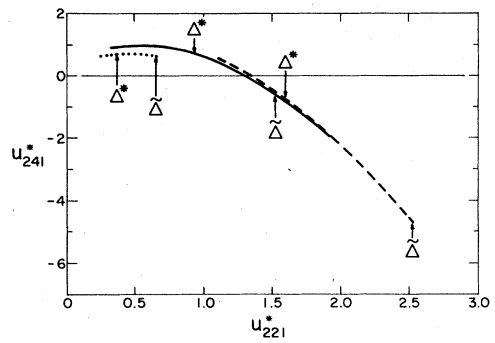

FIG. 5. Approximate line of Ising fixed points in terms of the parameters u^*_{221} and u^*_{241} as defined in Eq. (2.30). The different segments are generated by varying the spin-rescaling parameter Δ for three A values and truncations: $A=1$ and Trun(3,3,1) (dotted line), $A=2$ and Trun(4,4,1) (solid line), and $A=3$ and Trun(4,3,1) (dashed line). Marked are the locations of Δ^* and $\tilde{\Delta}$ within which $y_{221}<0$.

truncation by increasing n_0, n_{21}, or n_{41} by 1, with $n_{22}=n_{21}-1$. Compute y_{200} for the "new" truncation at the fixed point with $\Delta=\Delta^*$.

(3) Discard any "new" truncation for which aberrant behavior or no critical fixed point is found.

(4) Accept as the "new" balanced truncation the one with the largest change in y_{200} relative to the "old" truncation. If two or more truncations exhibit shifts of comparable magnitude, examine the shifts in η, and if these are also similar, accept both truncations as "new" balanced ones.

(5) Repeat steps (1)—(4) to generate a sequence of truncations until the balanced truncation includes the marker μ_{241} (i.e., $n_{41}=1$). Then, we assume, new balanced truncations require the presently unavailable scaling fields $\mu_{\bar{m}4l}$, $\mu_{\bar{m}61}$, etc.

2. *Choice of redundant normalization parameter A*

The results in Table I suggest that a range of A values exists that is optimal in the sense that it postpones the need for the scaling fields that are not available. Here we formalize this argument.

There are *two* ways of parametrizing the line of fixed points: either in terms of the scaling field μ^*_{221}, as was done in Sec. II B, or as function of the redundant parameter A, as will be done here. Both ways were discussed for the Gaussian fixed line in Eqs. (2.23)—(2.25). By comparing the Landau Hamiltonians (2.2) and (2.4), the functions $u_{\bar{m}}(\underset{\sim}{q}_1,\ldots,\underset{\sim}{q}_{\bar{m}};l)$ can be expressed in terms of the SF coordinates $\mu_{\bar{m}pt}(l)$ and homogeneous functions $f_{\bar{m}pt}\{\underset{\sim}{q}_i\}$ [see Eq. (2.14)]. For example, the small-q expansion of $u_2(q;l)$ is

$$u_2(q;l)=u_{200}(l)+u_{221}(l)q^2+u_{241}(l)q^4+\cdots . \quad (2.30)$$

Explicit formulas are derived in Appendix A. Note that the factors $\psi(q_i)$ in the definition (2.14) of $Q_{\bar{m}pt}[\sigma]$ contribute to $u_{\bar{m}}\{\underset{\sim}{q}_i;l\}$ to all orders in q, even when $p=0$. In this parametrization, the A dependence is completely absorbed in the definition of the set of q-independent coefficients $u_{\bar{m}pt}(l)$.

Now we show that the effects of the scaling fields that are unavailable can be reduced by minimizing, as a function of A, the fixed-point value of the coefficient u^*_{241} that is related to the marker scaling field μ^*_{241} through Eqs. (A3)—(A5) and (A13). (For generalization, see the end of this section.) Note that for the *Gaussian* fixed point, the small-q expansion of Eq. (2.10b),

$$u^*_G(q)=Aq^2+A(2-A)q^4+A(A^2-4A+2)q^6+\cdots , \quad (2.31)$$

indicates that for $A=2$ the coefficient of the quartic term vanishes. For the case of the Ising model ($N=1$), Fig. 5 exhibits the fixed-point values of $u^*_{241}(\Delta)$ versus $u^*_{221}(\Delta)$ for three values of A from three different truncations. The locations Δ^* and $\tilde{\Delta}$ are marked. Now considering $u^*_{221}(\Delta)$ [instead of $\mu^*_{221}(\Delta)$] as an independent variable that generates a (true) fixed line, we interpret the result as showing that different portions of the fixed line are mapped out when, for different A, Δ is varied in the range $\tilde{\Delta}\le\Delta\le\Delta^*$. We find the remarkable separation that, for all truncations, Δ^* is associated with positive values u^*_{241} when $A=1$ and 2, and negative values when $A=3$. That observation suggests that the importance of the q^4 contributions to the fixed-point Hamiltonian can be minimized by choosing A in an "optimal" range such that $u^*_{241}(\Delta^*)=0$ is bracketed. Results for $u^*_{241}(\Delta^*)$,

TABLE II. Fixed-point values of the expansion parameter u^*_{241} in Eq. (2.30) for $N=0,\ldots,3$ as functions of A for the largest balanced truncations studied. The optimal range of values of A is chosen to bracket $u^*_{241}=0$.

	$A=2$		$A=3$	
N	Truncation	u^*_{241}	Truncation	u^*_{241}
0	Trun(4,4,3,1)	0.586	Trun(5,4,3,0)	−0.213
			Trun(4,5,4,0)	−0.498
1	Trun(4,5,1)	0.683	Trun(4,5,1)	−0.607
			Trun(5,4,1)	−0.877
2	Trun(4,5,4,0)	0.820	Trun(5,4,3,0)	−0.827
3	Trun(4,5,4,0)	0.878	Trun(5,4,3,0)	−1.063

TABLE III. Parameters in reduced units characterizing the critical fixed-point potential $\tilde{W}(\tilde{\sigma})$ of Eq. (2.33) for Ising systems. Results for three truncations with $n_{eq}=10$ SF equations are shown.

Truncation	A	$\tilde{v}^*_{200}$	$\tilde{v}^*_{400}$	$\tilde{v}^*_{600}$	$\tilde{v}^*_{800}$	$\tilde{v}^*_{10,00}$
Trun(4,5,1)	2	−2.10	1.21	−0.19	0.003	
Trun(4,5,1)	3	−2.16	1.32	−0.18	0.009	
Trun(5,4,1)	3	−2.17	1.36	−0.20	0.017	−0.000 58

when $N=0,\ldots,3$ and the longest truncations studied, are given in Table II for $A=2$ and 3. A comparison with Table I shows that indeed the above choice of A yields the longest sequences of balanced truncations. When $A<2$ or $A>3$, the construction of balanced truncations requires the addition of the scaling field μ_{241} at an earlier stage.

We suppose that the idea of determining optimal A values by minimizing the "marker" fixed-point coefficient $u^*_{\bar{m}=2,p'+2,t=1}$ applies also to other levels of calculational precision. For short truncations that have available only the $p=0$ scaling fields (with the exception of μ_{221}), we minimize numerically the value of $u^*_{221}(\Delta^*)$. The criterion yields $A\approx 0.5$. Indeed, for this value of A we obtain the best results for the critical exponents for all small truncations and all A values studied. For this reason, $A=0.5$ was used for the estimation of critical exponents of the cubic and Potts models.[3,4] For an extended calculation involving longer truncations, i.e., those retaining all scaling fields $\mu_{\bar{m}pt}$ with $p\le p'$, but none with $p=p'+2$ except $\mu_{2,p'+2,1}$, we propose to minimize the coefficient $u^*_{2,p'+2,1}(\Delta^*)$ by appropriately choosing A.

3. *Stability of the fixed-point potential*

A different perspective on the concept of "balanced truncations" is provided by considering the boundedness and universality of the fixed-point potential associated with the approximate critical fixed points. We answer this question qualitatively by characterizing, as in Landau theory or Wilson's approximate RG approach, the thermodynamic potential in terms of the $q=0$ components of $H^*[\sigma]$. Using formulas derived in Appendix A, we parametrize $H^*[\sigma]$ in terms of the coefficients $v^*_m\{\underline{q}_i\}$ and expand those coefficients into the set of homogeneous functions $f_{\bar{m}pt}\{\underline{q}_i\}$. This defines a set of numbers $v^*_{\bar{m}pt}$, in terms of which, for $N=1$, the thermodynamic potential can be approximated:

$$W(\sigma_0)=v^*_{200}\sigma_0^2+v^*_{400}\sigma_0^4+v^*_{600}\sigma_0^6+\cdots, \tag{2.32}$$

with $\sigma_0\equiv\sigma(q=0)$. The *universality* of the shape of this potential may be examined by expressing Eq. (2.32) in reduced units, $\tilde{W}=W/W_{\min}$ and $\tilde{\sigma}=\sigma_0/\sigma_{\min}$, where $W_{\min}$ and $\sigma_{\min}$ denote the depths and location of the minimum of $W(\sigma_0)$,

$$\tilde{W}(\tilde{\sigma})=\tilde{v}^*_{200}\tilde{\sigma}^2+\tilde{v}^*_{400}\tilde{\sigma}^4+\tilde{v}^*_{600}\tilde{\sigma}^6+\cdots. \tag{2.33}$$

Numerical results for the parameters in Eq. (2.33) for $N=1$ are exhibited in Table III for three representative large truncations with $A=2$ and 3. In summary, we find the following:

(i) All truncations with odd numbers of equations n_0 [defined by Eq. (2.17)] have unstable (unbounded) potentials $\tilde{W}(\tilde{\sigma})$. This behavior is reflected in the signs of $\tilde{v}^*_{\bar{m}00}$ (shown in Table III), which alternate as function of $\bar{m}$.

(ii) The stable potentials have the form shown in Fig. 6; specifically, the figure shows the fixed-point potential for the Ising model for truncation Trun(4,5,1) with $A=2$.

(iii) The potential $\tilde{W}(\tilde{\sigma})$ of Eq. (2.33) approaches a universal form with increasing n_{eq}, when the sequences of truncations and optimal ranges of A are chosen as described in Secs. II C *1* and II C *2*. The values of $\tilde{v}^*_{200}$ and $\tilde{v}^*_{400}$ vary by less than 2% and 6%, respectively, for the balanced truncations with $6\le n_{eq}\le 10$ for $A=2$ and 3. The absolute value of $\tilde{v}^*_{\bar{m}00}$ decreases rapidly with increasing $\bar{m}>4$ (see Table III).

(iv) The depth of the minimum of the potential, $W_{\min}$, and the square of its width, $\sigma^2_{\min}$, scale roughly as $1/A$, in agreement with Eq. (2.23).

On a more quantitative level, the fixed-point Hamiltonian is a *functional* of the spin variables $\vec{\sigma}(q)$ and, therefore, the $q\neq 0$ contributions must be included in the consideration of boundedness. For a quick overview, it is convenient to parametrize the other fixed-point coordinates likewise in terms of the set of numbers $\tilde{v}^*_{\bar{m}pt}$. We find that the pattern of alternating sign of $\tilde{v}^*_{\bar{m}00}$ as function of $\bar{m}$ is repeated for $\tilde{v}^*_{\bar{m},p=2,t}$. Furthermore, we note that no large ($n_{eq}>7$) balanced truncation has been found for which more than one of the numbers n_{pt} [defined by Eq. (2.17)] is odd. Truncation Trun(5,4,1) in Table III is an example of a truncation that is unstable for large $\tilde{\sigma}$, but, due to the $p>0$ contributions, is sufficiently balanced so that its potential for small $\tilde{\sigma}$ differs only insignificantly from those of neighboring truncations. On the other hand, truncations such as Trun(5,5,4,0) are always unbalanced and often so aberrant that *no* fixed point can be found for $N=0$ to 3. In summary, the truncated form of

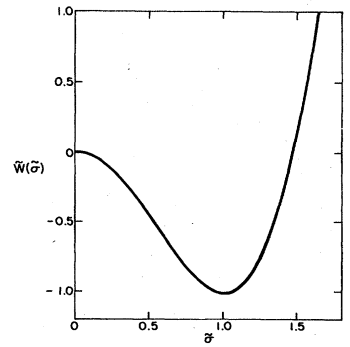

FIG. 6. Critical fixed-point potential for the Ising model. Results are for Trun(4,5,1) with $A=2$.

the SF equations (2.5) is sensitive to the criterion of boundedness of the fixed-point potential. We expect this issue to become more important at the higher levels of approximation.

4. *Approximations with $p' \geq 4$*

The study of sequences of balanced truncations that include scaling fields with $p' \geq p = 4$ awaits the computation of the associated coupling coefficients a_{mjk}. However, even the extension for the Ising model ($N = 1$), which is the simplest nontrivial calculation at the next level in p, is not easy. There are three linearly independent operators of the type $p = 4$ for $N = 1$; the corresponding homogeneous functions $f_{\bar{m}4t}\{q_i\}$ are listed in Appendix E of I. We summarize here possible changes in the computational procedures necessary to implement the next levels of calculation.

(i) Determination of coupling coefficients a_{mjk}. As outlined in I [see Eq. (4.21) of that reference], the a_{mjk} are generally sums of products of combinatorial factors and of integrals. As mentioned there and in Ref. 3, algebraic-manipulation computer routines will aid in deriving the analytical expressions as functions of N for the momentum and spin combinatorics. The dependence of the a_{mjk} on the spatial dimension d originates from the integrals. Their computation for the extended calculations should not pose significant difficulties since all integrals encountered can be expressed as one-dimensional integrals by using Fourier-transform techniques.[1]

(ii) Numerical precision. The precision of the numerically determined integrals, currently 1 part in 10^5, may need to be increased. We tested for the propagation of error from the integrals to the critical exponents by measuring the effect of an additional larger random error added to each integral. Currently, Control Data Corporation double-precision (120-bit) routines were necessary only for computing the Fourier transforms that enter each integral. It is possible that quadruple precision will be required for extended calculations.

(iii) Locating fixed points for large n_{eq}. The clearest procedure for finding a fixed point is through RG flow (see Sec. II B of I). Since this method is time consuming, we usually reserved it for checks when other procedures failed. Instead, the fixed-point coordinates of the preceding truncation are used as input to a routine based on Newton's method.[26]

(iv) Adding sets of scaling fields. There are two cases when one may need to add sets of scaling fields, rather than a single scaling field, when increasing the length of the truncation. First, we always add simultaneously scaling fields $\mu_{\bar{m}pt}$ that differ only by the index t. This is because the structure of the coefficients a_{mjk} causes the new SF equations $d\mu_{\bar{m}pt_1}/dl$, $d\mu_{\bar{m}pt_2}/dl$, etc. to couple to the old ones in a similar way. Second, the tendency of balanced truncations to have bounded or almost bounded fixed-point potentials implies that the larger balanced truncations will have all or most of the n_0, n_{21}, n_{41}, etc. even (for details, see Sec. II C 3).

(v) Using μ^*_{221} as the free parameter. As evidenced in Figs. 1(b) and 2(b), the line of fixed points as a function of μ^*_{221} is localized to a range of Δ that approximates the discrete value Δ^*_e. Since, for large truncations, this range in Δ can be smaller than the fluctuations of Δ^* as a function of n_{eq}, it may be easier to treat μ^*_{221} as the free parameter, rather than Δ, and determine $\Delta(\mu^*_{221})$, rather than $\mu^*_{221}(\Delta)$.

(vi) Determination of A. For the extended calculation, the parameter A must be redetermined such that the largest sequences of balanced truncations are obtained. As described in Sec. II C 3, we expect one should choose A values that bracket $u^*_{2,p'+2,1} = 0$. It is possible that more than one range of A values exists with that property. This is indicated by the result for the Gaussian fixed point that the $u^*_{G;2p1}$ with $p \geq 6$ depend nonlinearly on A [e.g., $u^*_{G;261}$ in Eq. (2.31) is quadratic in A]. In addition, the idea that the choice of A becomes less stringent for extended calculations is consistent with the notion of universality.

III. DETERMINATION OF CRITICAL EXPONENTS FOR THREE DIMENSIONS

In this section the SFM is applied to the high-precision calculation of the critical exponents of the isotropic N-

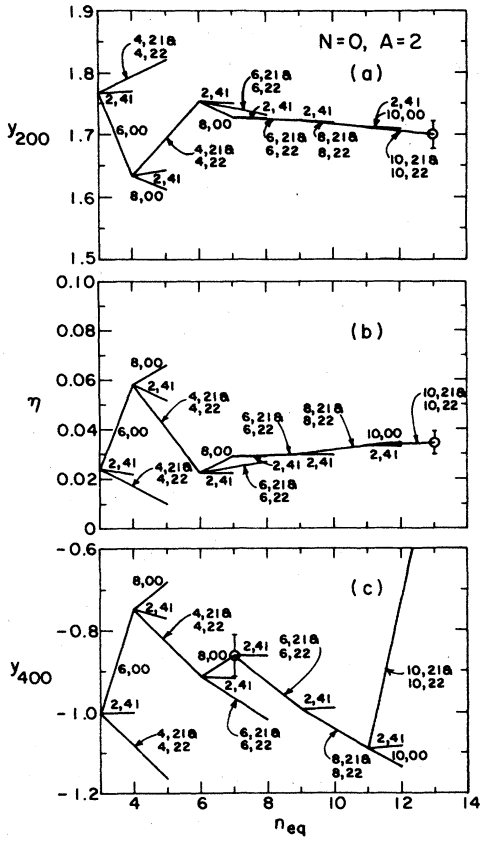

FIG. 7. Critical exponents of the isotropic N-vector model with $N = 0$ from sequences of balanced truncations to the SF equations. Shown are (a) thermal exponent y_{200}, (b) correlation-function exponent η, and (c) correction-to-scaling eigenvalue y_{400} versus the number n_{eq} of SF equations for truncations with $A = 2$. The labels on the line segments are explained in the caption of Fig. 4 and in the text.

vector model with $N=0$, 1, 2, and 3. New results for several correction-to-scaling exponents are obtained. The evaluation of the quality of the exponent estimates and comparisons with other methods are deferred to Sec. IV. The limit of large N is also considered and results compared with exact analytical information.

A. Critical exponents ν and η

In the SF approach, estimates for the values of critical exponents and their confidence limits are obtained by studying *sequences* of balanced truncations. The self-consistent generation of such sequences has been described in Sec. II C. Rough estimates for exponents can be produced by considering one or two specially selected truncations, as was done, e.g., in Refs. 3 and 4. In high-precision work, both the length of the truncation, n_{eq}, and the value of the redundant parameter, A, are varied systematically. This procedure leads to unbiased estimates for the values of critical exponents and to confidence limits that include systematic errors due to truncation.

Consider first the raw data. For the isotropic N-vector model with $N=0$, 1, 2, and 3, Figs. 7–10 display the results for the exponents y_{200}, η, and y_{400} as functions of the total number of SF equations n_{eq} for $A=2$. Similar results are obtained for the parameter value $A=3$; see, for example, Fig. 4, which exhibits for the Ising model ($N=1$) the corresponding y_{200} and η versus n_{eq}. In the figures the labels on the connecting lines denote the indices $m=\{\bar{m},p,t\}$ of the scaling field(s) last added to the truncation, and the continuous lines trace the exponent values of the respective sequences of balanced truncations. The sequences for $N\neq 1$ are identical with the ones in Table I for $N=1$ with the following exception: At $n_{eq}=12$ with $A=3$, the balanced truncation for $N=0$, 2, and 3 is Trun(5,4,3,0). Two minor modifications in the procedures are made when $N\neq 1$. The scaling fields $\mu_{\bar{m}21}$ and $\mu_{\bar{m}22}$ are always added simultaneously and, since coupling coefficients a_{mjk} with $\bar{m}>5$ have not been computed, the sequence of balanced truncations is stopped when the scaling fields μ_{241}, $\mu_{10,00}$, or $\mu_{10,21}$ *and* $\mu_{10,22}$ are added.

By examing the sizes and signs of the shifts in y_{200} and η when new scaling fields $\mu_{\bar{m}pt}$ are added to the truncations, one finds the following patterns in the fluctuations of critical exponents as functions of n_{eq}. (The

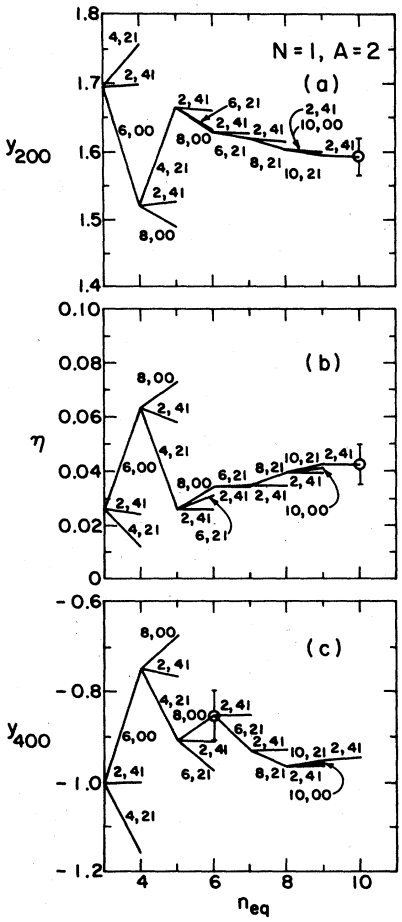

FIG. 8. Critical exponents (a) y_{200} (thermal), (b) η (correlation function), and (c) y_{400} (correction-to-scaling eigenvalue) of the isotropic N-vector model with $N=1$ versus the number n_{eq} of SF equations for truncations with $A=2$. For details, see caption of Fig. 7.

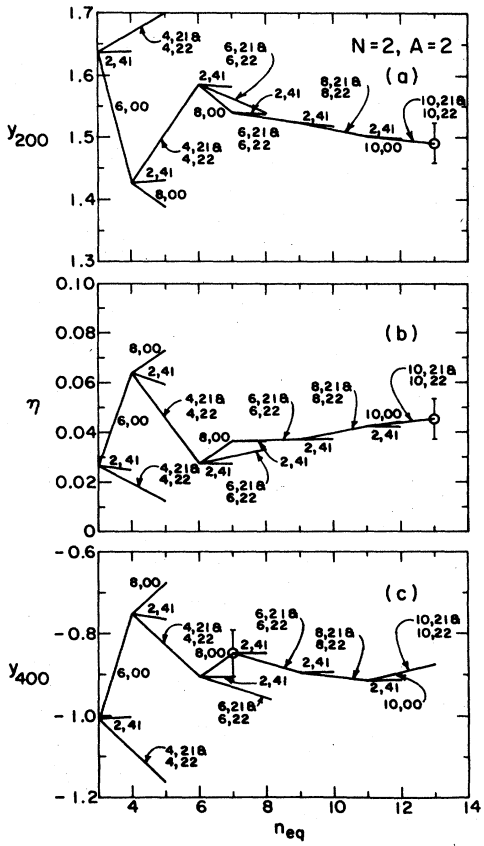

FIG. 9. Critical exponents (a) y_{200} (thermal), (b) η (correlation function), and (c) y_{400} (correction-to-scaling eigenvalue) of the isotropic N-vector model with $N=2$ versus the number n_{eq} of SF equations for truncations with $A=2$. For details, see caption of Fig. 7.

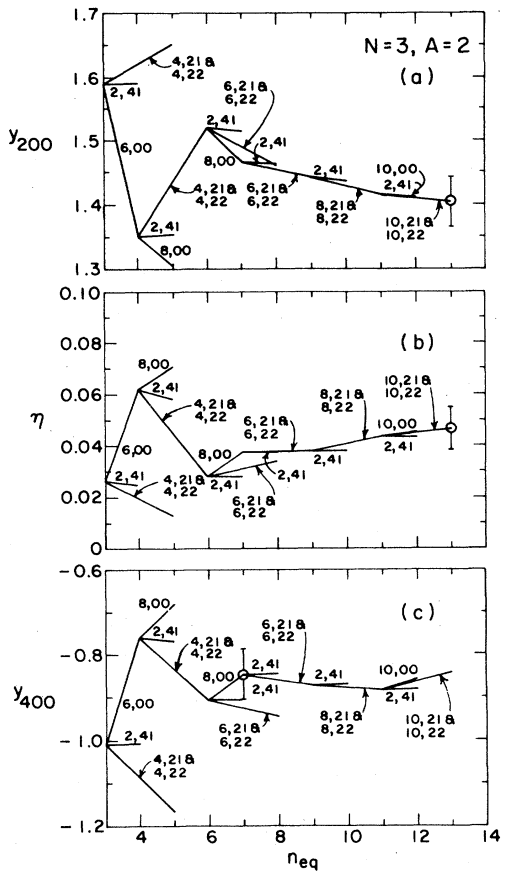

FIG. 10. Critical exponents (a) y_{200} (thermal), (b) η (correlation function), and (c) y_{400} (correction-to-scaling eigenvalue) of the isotropic N-vector model with $N=3$ versus the number n_{eq} of SF equations for truncations with $A=2$. For details, see caption of Fig. 7.

correction-to-scaling eigenvalue y_{400} is discussed separately in Sec. III B.) The general pattern of y_{200} and η versus n_{eq} in Figs. 4 and 7—10 is *oscillatory* for small n_{eq} and *smooth* for $n_{eq}\geq 9$ (or 7, when $N=1$). In general, the scaling fields $\mu_{\bar{m}00}$ and $\mu_{\bar{m}21},\mu_{\bar{m}22}$ cause shifts in opposite directions. The absolute value of these shifts decrease with increasing $\bar{m}$ until $n_{eq}=9$ (or 7, when $N=1$). The addition of this pair of scaling fields marks the beginning of the smooth regime. The shifts caused by $\mu_{\bar{m}00}$ compared with those of $\mu_{\bar{m}21},\mu_{\bar{m}22}$ are larger at small $\bar{m}$ and become of about the same size for $\bar{m}=10$. We suppose that this latter pattern continues when scaling fields $\mu_{\bar{m}pt}$ with $p>2$ are added, which would be consistent with the structure of the stability matrix $Y(m,j)$ discussed in Sec. II C *1*. Presumably, the scaling fields $\mu_{\bar{m}4t}$ will cause shifts of the same sign as $\mu_{\bar{m}00}$. The size of the shifts, we expect, should be smaller at small $\bar{m}$ than those due to $\mu_{\bar{m}00}$ or $\mu_{\bar{m}2t}$, decrease with increasing $\bar{m}$, and approach in size the shifts caused by $\mu_{\bar{m}00}$ or $\mu_{\bar{m}2t}$ just prior to the addition of the marker μ_{261}.

We determine estimates of the critical exponents ν and η and their confidence limits from the sequences of balanced truncations in the following way. We assume that the existence of the smooth regime in the plots of y_{200} and η versus n_{eq} indicates that the exponents have begun to settle towards their universal values. Thus, for each number of spin components N and value of the parameter A, we take the values of $\nu=1/y_{200}$ and η to be those of the largest balanced truncation available (typically, $n_{eq}=13$, for $N\neq 1$, and $n_{eq}=10$, for $N=1$). Then we define confidence limits by the width of the "window" that contains all values of critical exponents obtained within the smooth regime, $n_{eq}\geq 9$ (or 7, for $N=1$). Typical results are shown in Figs. 4 and 7—10 for the parameter choices $A=2$ and 3. Varying A at large n_{eq} leads to small vertical shifts in the curves. (Compare Figs. 4 and 8, for example.) Typical results for the variation of the critical exponents with A are shown in Table IV for $N=1$ for $A=2$ and 3. (The choice of A values is discussed in Sec. II C *2*.) To obtain the results shown in Table V, we average the results obtained for $A=2$ and 3, weighted by the squares of the inverse of the confidence limits. Since there are presumably correlations between data for $A=2$ and 3, our cumulative confidence limits of Table V represent error estimates obtained by averaging the square of the confidence limits. In addition, when there is more than one balanced truncation for a given value of A, those results are similarly averaged before averaging results for $A=2$ and 3. Results for other critical exponents, such as

TABLE IV. Critical exponents of the Ising model and their confidence limits from the largest sequences of truncations with $A=2$ and 3. Exponents y_{400} are determined from shorter truncations for reasons described in Sec. III B 2. Averaging of results yields the exponent values in Table V for $N=1$.

Exponent	Truncation	A	Value	Confidence limits
ν	Trun(4,5,1)	2	0.6283	0.0104
ν	Trun(4,5,1)	3	0.6252	0.0063
ν	Trun(5,4,1)	3	0.6259	0.0071
η	Trun(4,5,1)	2	0.0423	0.0075
η	Trun(4,5,1)	3	0.0384	0.0050
η	Trun(5,4,1)	3	0.0389	0.0055
y_{400}	Trun(4,2,0)	2	−0.853	0.056
y_{400}	Trun(4,2,0)	3	−0.860	0.095

TABLE V. Critical exponents of the isotropic N-vector model in three dimensions calculated by the scaling-field method in an approximation using balanced truncations that include up to 13 equations. The correction-to-scaling exponents Δ_m are defined by $\Delta_m = -\nu y_m$. For $N=1$, the "even" eigenvalue y_{421} is unphysical and not shown, while the "odd" eigenvalue y_{500} is of interest for the liquid-gas transition. Confidence limits include systematic errors due to truncation.

	$N=0$	$N=1$	$N=2$	$N=3$
ν	0.585±0.005	0.626±0.009	0.672±0.015	0.715±0.020
η	0.034±0.005	0.040±0.007	0.043±0.007	0.044±0.007
γ	1.15 ±0.01	1.23 ±0.02	1.31 ±0.02	1.40 ±0.03
$-y_{400}$	0.87 ±0.06	0.855±0.07	0.85 ±0.07	0.84 ±0.07
$-y_{421}$	1.68 ±0.08		1.77 ±0.07	1.78 ±0.11
$-y_{422}$	1.83 ±0.17	1.67 ±0.11	1.79 ±0.07	1.98 ±0.05
$-y_{500}$		2.4 ±0.4		
Δ_{400}	0.51 ±0.04	0.54 ±0.05	0.57 ±0.06	0.60 ±0.07
Δ_{421}	0.98 ±0.06		1.19 ±0.07	1.27 ±0.11
Δ_{422}	1.07 ±0.11	1.05 ±0.08	1.20 ±0.07	1.42 ±0.08
Δ_{500}		1.5 ±0.3		

α, γ, or δ, can be obtained using the usual exponent relationships. The result for γ, shown in Table V, is obtained by applying the relationship $\gamma=\nu(2-\eta)$ directly to the sequence of balanced truncations, and thus takes into account correlations in shifts of y_{200} and η.

Our method of determining critical exponents and confidence limits is inevitably somewhat subjective, although it is based on a "blind-folded" procedure (see Sec. II C *1*). Our confidence limits are chosen based on a pattern of shifts of the exponents due to scaling fields of types $\mu_{\bar{m}00}$, compared with $\mu_{\bar{m}pt}$, that were discussed above. We have assigned symmetric confidence limits, thus ignoring the overall trends as functions of $n_{\rm eq}$ of y_{200} (decreasing) and η (increasing). In fact, given the trends in y_{200} and η versus $n_{\rm eq}$, one needs to worry that the exponent values "overshoot," which would explain the somewhat low value of the critical exponent $\gamma=\nu(2-\eta)$ given in Table V. The procedure can be tested at the next level of approximation (see Sec. II C *4*) by adding scaling fields of types $\mu_{\bar{m}4t}$, thus checking the predictions for the pattern of the exponents as functions of $n_{\rm eq}$ and $m=\{\bar{m},p,t\}$. The reader can judge our procedure for determining exponents and confidence limits by using the evidence presented in Figs. 4 and 7 and Tables IV and V.

We defer a comparison of the results in Table V to those by other techniques to Sec. IV. In the following we discuss the determination of the other entries in the table.

B. Correction-to-scaling exponents

1. Overview

The universal correction-to-scaling exponents characterize the critical behavior of thermodynamic and correlation functions beyond the asymptotic terms.[8] Recently, the estimation of those exponent values is attracting much interest. In the analysis of HT series, the leading correction exponent[20] Δ_{400} is incorporated into the fitting procedure through a confluent singularity term. The discussion of experimental data usually requires the values of correction exponents as input parameters. FT expansion techniques and the MC renormalization group have also been used to determine the exponent Δ_{400}, although results from the latter[17] are unsatisfactory at present. For further details, see Sec. IV.

The SFM is ideally suited for the estimation of several of the correction exponents Δ_m since they are defined in terms of the lower-lying irrelevant eigenvalues of the matrix (2.8). However, there are two difficulties inherent in that procedure. First, the set of basis operators is overcomplete and some of the irrelevant eigenvalues may be either nonphysical or redundant, in the sense of Wegner.[22,24] Their identification at the critical fixed point is not easy. Second, correction-to-scaling eigenvalues sometimes cross as a function of N. In truncations, one finds that when eigenvalues are too close they can form complex pairs for some interval of N. This can significantly affect the precision to which the eigenvalues can be determined. In the following we address these questions, first for the exponents of the "even" or O(N)-symmetric operators for $N=0,\ldots,3$, and second, for the exponents of the "odd" or symmetry-breaking operators for $N=1$.

2. Even correction-to-scaling exponents

In Fig. 11, which exhibits the portion of the spectrum of "even" eigenvalues as functions of N as obtained from Trun(4,4,3,1) with $A=1$, the eigenvalues that are nonphysical are indicated by two dots. For example, in the exact Gaussian limit $N=-2$, certain operators decouple from the set of physical operators (see Appendix B for details) and do not contribute to a calculation of the free energy. (Among those nonphysical eigenvalues is y_{400}; in-

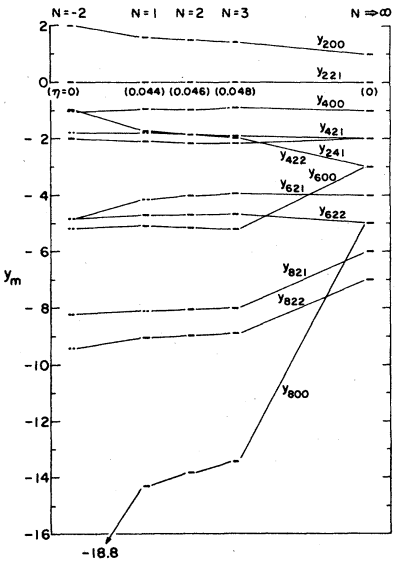

FIG. 11. Spectrum of eigenvalues as function of N of the critical fixed point of the isotropic N-vector model from Trun(4,4,3,1) with $A=1$. Nonphysical eigenvalues are indicated by two dots.

y_{400}; instead, $y_{422}=-1$ provides the first correction-to-scaling exponent when $N=-2$.) Similarly, for $N=1$, the SF basis set is overcomplete and all eigenvalues $y_{\bar{m}21}$ are recognizable as being nonphysical (see comments in Sec. III B of I). In the limit $N\to\infty$, the set of basis operators is smaller than for $N<\infty$, but the nonphysical eigenvalues $y_{\bar{m}pt}$ coincide in value with the physical eigenvalues $y^{\rm sph}_{\bar{m}pt}$ (see Sec. V B of I for details). Redundant eigenvalues[22,24] are identifiable by invariances of the Landau Hamiltonian under the RG transformation. The only "even" redundant eigenvalue that we have identified is the marginal eigenvalue y_{221} (see Sec. II of I), which is associated with the transformation (2.23). (Redundant "odd" eigenvalues are discussed in the next subsection.)

Figure 12 illustrates the problems inherent in calculating the correction-to-scaling exponents from irrelevant eigenvalues y_m that cross as functions of N. We show in this figure typical behaviors of these eigenvalues for small and large truncations (dashed and solid lines, respectively). The labeling of the eigenvalues is discussed at the end of Sec. II A. For small truncations, i.e., $n_{21}\le 2$, no scaling fields $\mu_{\bar{m}pt}$ with $\bar{m}>4$ are included in the truncation; then y_{421} and y_{422} are the last eigenvalues of the block 2-2 of the determinant shown schematically in Fig. 3. For $n_{21}>2$, the eigenvalues y_{421} and y_{422} are immersed in the block 2-2 and are found closer in value to y_{400}. When the eigenvalues are too closely spaced, they tend to form complex pairs. (In the figure, only the real parts of the eigenvalues are shown.) The range of N over which complex pairs of eigenvalues are found is truncation dependent. *Outside* the range of complex-pair formation, the eigenvalues that form complex pairs are curved as a function of N. For example, this causes larger systematic errors in y_{400} when determined from Trun(5,4,3,0) at $N=0$ and 1 than at $N=3$. This kind of observation one is only able to make in methods in which N can be varied continuously. Presumably, the existence in our calculation of complex pairs of eigenvalues is an artifact of truncation, although, for noninteger N, the formation of complex pairs is not excluded on physical grounds. We believe that this difficulty can be removed by including scaling fields of the types $\mu_{\bar{m}pt}$ with $p\ge 2$. Then there will be new eigenvalues $y_{\bar{m}pt}$ that are close in value to y_{421} and y_{422}, and if any complex pairs are found, hopefully they will be at lower levels of the spectrum.

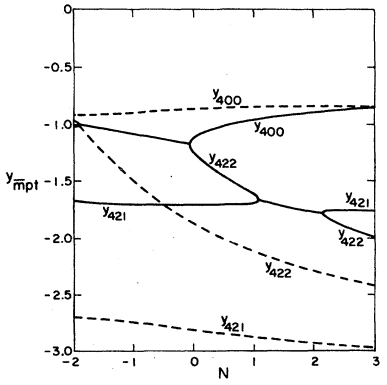

FIG. 12. Correction-to-scaling eigenvalues y_{400}, y_{421}, and y_{422} of the isotropic N-vector model as functions of N from truncations Trun(5,4,3,0) (solid lines) and Trun(4,2,1,0) (dashed lines) with $A=2$. When eigenvalues cross, they may form complex pairs, indicated in the figure by the joining of two lines.

The graphs of y_{400} as functions of $n_{\rm eq}$ in Figs. 7(c)–10(c), for $N=0$ to 3, reflect the above complications. Compare, in particular, Figs. 7(c) and 10(c). For $N=0$, y_{400} versus $n_{\rm eq}$ exhibits a strong downward trend for $n_{\rm eq}>7$ and a lack of settling towards an asymptotic value. For $N=3$, in contrast, y_{400} versus $n_{\rm eq}$ exhibits oscillatory and smooth regimes resembling those found in y_{200} or η as functions of $n_{\rm eq}$. Since the aberrant behavior is probably due to truncation (i.e., the complex pair of y_{400} with y_{422} when $n_{\rm eq}>7$ and $N<0$, as shown in Fig. 12), we determine for *all* N the first correction-to-scaling eigenvalue y_{400} as follows. We ignore all values of y_{400} obtained for $n_{\rm eq}>7$ and estimate y_{400} by the value of the largest truncation for which all eigenvalues are real, i.e., Trun(4,2,1,0). The estimates of y_{400} so determined are shown by circles in Figs. 7(c)–10(c). We estimate the confidence limits on these values for y_{400} by the size of the shifts relative to the previous balanced truncation. This confidence limit is conservative for $N=3$ [see Fig. 10(c)], but may not be large enough for $N=0$ and 1, where less trustworthy information is available. In this way, exponent values are determined for each sequence of balanced truncations and then averaged. The results are summarized in Table V. Finally, the estimates for Δ_{400}, as shown in Table V, are computed from the results for ν and y_{400} in the table. Our derivation of these estimates stresses the influence of lower-lying eigenvalues on the precise calculation of the leading correction-to-scaling eigenvalues.

The next-to-leading correction-to-scaling eigenvalues y_{421} and y_{422} are estimated as follows. Returning to Fig.

TABLE VI. Consistency check of the scaling-field method for the computation of critical exponents using relationship (3.1b) between the exponents y_{321}, y_{200}, and η. Last two columns show the numerical results for y_{321} and percentage deviations from equality for the balanced truncations with $n_{eq}=8$, 9, and 10.

n_{eq}	Truncation	A	y_{321}	Deviation (%)
8	Trun(4,4,0)	2	−0.840	4.3
	Trun(4,4,0)	3	−0.819	6.9
9	Trun(4,5,0)	2	−0.874	1.3
	Trun(4,5,0)	3	−0.858	3.6
	Trun(5,4,0)	3	−0.819	7.9
10	Trun(4,5,1)	2	−0.880	0.8
	Trun(4,5,1)	3	−0.868	1.5
	Trun(5,4,1)	3	−0.826	6.5

12, we note first that the relative ranking of these eigenvalues is truncation dependent. For short truncations, ones in which y_{421} and y_{422} are the last added eigenvalues in block 2-2, we find $y_{421}<y_{422}$ for *all* small N (i.e., $-2\leq N\leq 3$), while for larger truncations, i.e., ones in which these eigenvalues are immersed in the block 2-2, we find $y_{421}>y_{422}$ for $N\gtrsim 2$. Presumably the latter ranking is the correct one for $N\gtrsim 2$. Second, it is evident that the formation of complex pairs affects the estimation of y_{422} at $N=0$ more than that of y_{421} at $N=0,\ldots,3$ and y_{422} at $N=1$, 2, and 3. Therefore we estimate y_{422} at $N=0$ as described above for y_{400} and the other eigenvalues as described in Sec. III A for y_{200} and η. Owing to this difference in procedure at $N=0$, we quote $y_{421}>y_{422}$ in Table V, although we expect $y_{421}<y_{422}$ (as shown in Fig. 12). For $N=1$, the eigenvalue y_{421} is unphysical (see Sec. II A). To summarize, for $N=1$, there is *one* correction-to-scaling exponent, Δ_{422}, located at approximately $2\Delta_{400}$, while, for $N=0$, 2, and 3, there are *two* correction-to-scaling exponents, Δ_{421} and Δ_{422}, with $\Delta_{421}\neq\Delta_{422}$, located at approximately $2\Delta_{400}$.

3. *Exponents of symmetry-breaking terms for N=1*

Two important physical examples of Ising phase transitions are seen in liquid-gas and binary-fluid mixtures.[27] Model Landau Hamiltonians for those include both even and odd powers in $\sigma(q)$ in the expansion (2.2). The location of the critical fixed point is unchanged, i.e., the fixed-point coordinates of all "odd" scaling fields are zero (see Sec. IV B of I). However, *new* corrections to scaling for the critical transition originate from operators formed from odd powers in $\sigma(q)$.

Two of the three leading "odd" eigenvalues of the critical fixed point are associated with operators that are redundant.[22,24,28] All three are related to the correlation-function exponent η, and one is related to the thermal exponent y_{200}. The leading magnetic eigenvalue y_{100} is given by Eq. (2.22), while

$$y_{300}=\tfrac{1}{2}(d-2+\eta)\ , \tag{3.1a}$$

$$y_{321}=\tfrac{1}{2}(2y_{200}-5+\eta)\ . \tag{3.1b}$$

Thus these exponent relationships allow one to test the consistency of the SF calculation. We find that the relations for y_{100} and y_{300} can be satisfied exactly when compatible "even" and "odd" truncations are chosen. That is, in analogy to Eq. (2.18), we determine the numbers n'_0 and n'_{21} of the operators $Q_{\bar{m}'00}[\sigma]$ and $Q_{\bar{m}'21}[\sigma]$, where $\bar{m}'$ is an odd integer, that need to be included in the SF expansion (2.4) in order to properly reproduce the redundant operator associated with y_{300} at the critical fixed point. Wegner[22,24] has shown that this operator is related to the spin-shift operator $\delta H^*/\delta\sigma(q)$, which can be defined using a generalized Taylor-series expansion in $\sigma'(q)$ about the critical fixed point,

$$H^*[\sigma+\sigma']=H^*[\sigma]+\int_q \sigma'(q)\frac{\delta H^*}{\delta\sigma(q)}+\cdots\ . \tag{3.2}$$

Both the eigenvector associated with this operator and the eigenvalues y_{100} and y_{300} are obtained correctly when we use $n'_0=n_0$ and $n'_{21}=n_{21}-1$. Truncations that preserve relations for y_{100} and y_{300}, however, do not simultaneously satisfy Eq. (3.1b).[29] However, as shown in Table VI the degree of agreement found using Eq. (3.1b) is excellent, with deviations from equality usually decreasing with increasing n_{eq}.

The eigenvalue y_{500} provides the first new correction to

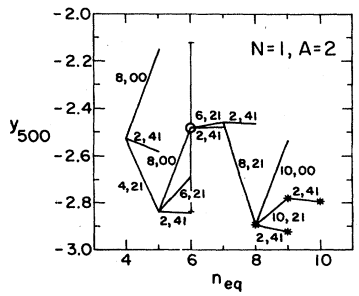

FIG. 13. "Odd" correction-to-scaling eigenvalue y_{500} of the Ising model versus the number n_{eq} of *even* SF equations for truncations with $A=2$. The labels $\{\bar{m},p,t\}$ on the line segments denote the *even* scaling fields added to the preceding balanced truncation. Asterisks indicate complex pairs with y_{521}.

scaling for liquid-gas or binary-fluid mixtures. This eigenvalue has not been calculated with any accuracy in ϵ expansion: Padé approximants for Δ_{500} from series to $O(\epsilon^2)$ yielded for $d=3$ an estimate $0.5 \leq \Delta_{500} \leq 1.0$,[27] and from series to $O(\epsilon^3)$, $\Delta_{500} \geq 1.0$.[30] Figure 13 shows the SF results for the eigenvalue y_{500} as a function of n_{eq} for the sequence of balanced truncations for $A=2$. A complex pair of y_{500} with y_{521} is found for $n_{eq}>7$. The result for $\Delta_{500}=1.5\pm0.3$ quoted in Table V is thus obtained as described for y_{400} (see Sec. III B *2*). We note that this correction-to-scaling exponent is roughly of size $3\Delta_{400}$.

C. Limit of large N

We have tested the SFM in the limit of large N by comparing numerical results for critical exponents with the analytical results:

$$\eta = cN^{-1} + O(N^{-2}) , \tag{3.3a}$$

$$y_{200} = 1 + 4cN^{-1} + O(N^{-2}) , \tag{3.3b}$$

$$y_{400} = -1 + 8cN^{-1} + O(N^{-2}) , \tag{3.3c}$$

where $c = 8/(3\pi^2) \simeq 0.2702$.[31] Exact results for η and all eigenvalues $y_{\bar{m}pt}$ in the spherical-model limit $N \to \infty$ have been obtained analytically by the SFM (for details, see Sec. V B of I). Here we use the methods developed in Sec. II to test the effects of truncation on numerically determined critical exponents. We calculate the eigenvalues y_{200}, y_{400}, and η in the spherical-model limit using $N=10^{20}$ and estimate the $1/N$ corrections in Eqs. (3.3) using $N=2^{15}$. The computation of these corrections provides a severe test of the method, due to the large precision necessary to determine c from numerical values of y_{200}, y_{400}, and η.

Since both numerical and analytical SF calculations of the spherical-model critical exponents yield exact results, one might expect that the $1/N$ corrections of Eqs. (3.3) are also easily obtainable from the SFM. This proved false, for a number of reasons, which we now list.

(i) Location of the fixed point. The SFM uses a parametrization that is different from that of other techniques, i.e., the SF expansion (2.4) about the Gaussian fixed point. This expansion can be troublesome if the fixed point of interest is located "far" from the Gaussian one in the SF coordinate space, as is the case for the spherical-model fixed point. After rescaling the scaling fields μ_m, operators $Q_m[\sigma]$, and coupling coefficients a_{mjk} and a_{mj} by the appropriate powers of N, so that the renormalized coupling constants are defined in the limit $N \to \infty$ (see Sec. V B of I), we still find large SF fixed-point coordinates, e.g., with $A=2$, $\tilde{\mu}^*_{200}=0$, $\tilde{\mu}^*_{400} \approx 1.6$, $\tilde{\mu}^*_{600} \approx -18$, and $\tilde{\mu}^*_{800} \approx 483$.

(ii) False fixed-line behavior at $N=\infty$. Because of the disparity between the Gaussian and spherical-model fixed points, exact SF results in the limit of $N=\infty$ can only be obtained for the "gauge" choice, or location on the line of fixed points, $\mu^*_{221}=0$. (This is in contrast to the Gaussian limit $N=-2$, where the line of fixed points can be studied exactly, as discussed in Appendix B.) In numerical work, where μ^*_{221} is not a free variable, the parameter r of Eq. (2.29), which measures the degree of correlation between the marginal eigenvector $\vec{t}$ to the vector $\vec{\lambda}^*$, is found to be $r \approx 0.87$. As for small N, truncated sets of SF equations yield exponents that exhibit a false dependence on the variable Δ. Figure 14 shows $-y_{221}$ as a function of Δ determined from the truncation Trun(4,4,3,1) with $A=2$ at $N=10^{20}$. The spherical-model eigenvalues are obtained when $y_{221}=0$, i.e., at the cusp $\Delta^*=0$.

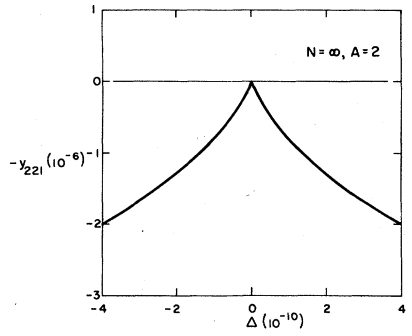

FIG. 14. "False" line of fixed points for $N=\infty$. Negative of the near-marginal eigenvalue, $-y_{221}$, versus Δ, shows the effect of truncation to Trun(4,4,3,1) with $A=2$.

(iii) False fixed-line behavior at large N. Behavior similar to that at $N=\infty$ is found for large N. Typically, the eigenvalue $-y_{221}$, when plotted as function of Δ, shows either cusps, as shown in Fig. 14, or, more rarely, "loops," as shown in Fig. 1(c). When cusps are found, then $y_{221}>0$, for all Δ. When loops are found, then their width $\delta\Delta$ is much smaller than the size of Δ^*, $\delta\Delta/\Delta^* \lesssim 0.1$.

These behaviors makes calculations difficult for large values of N.

In the following we summarize the differences in procedure for calculations at large and small N:

(i) Δ^* determination. We relax the procedures described in Sec. II by accepting into our data analysis truncations with cusplike diagrams of y_{221} versus Δ when, at the cusp, $y_{221} < 10^{-5}$. We then define Δ^* to be the value of Δ at the cusp.

(ii) Optimal value of A. We find that the longest balanced truncation at large N is shorter than that at small N. For example, for $N=2^{15}$, a relatively long sequence ending in Trun(4,4,3,0) is found, when $A=3$, and a much shorter one ending in Trun(3,2,1,0), when $A=2$. We choose $A=3$ as the optimal value of A for no other reason than that it yields the longest sequence of balanced truncations.

(iii) Sequences of truncations. For each truncated set of SF equations, we calculate c in three ways using Eqs. (3.3). Table VII tabulates the results for the largest sequences of truncations with $A=3$. Observing that the scaling field μ_{241} causes very large shifts in the $1/N$ correction to y_{200} (but not in those to η and y_{400}), we stop the sequence of balanced truncations at a level that excludes μ_{241}.

Table VII presents the results from the balanced truncations of $A=3$. For truncations with $3 \leq n_{eq} \leq 9$, the $1/N$

TABLE VII. Determination of $1/N$ corrections for the isotropic N-vector model using Eqs. (3.3) with $N=2^{15}$ by the scaling-field method at $A=3$. Shown are the largest balanced truncations (underlined) and numerical results for c obtained via the three relations (3.3). Asterisks indicate truncations exhibiting cusp behavior as described in Sec. III C.

n_{eq}	Truncation	c_η	c_{200}	c_{400}
9	Trun(4,3,2,0)*	0.29	0.10	0.48
10	Trun(4,3,2,1)*	0.29	0.13	0.48
10	Trun(5,3,2,0)*	0.29	0.29	0.17
11	Trun(4,4,3,0)	0.29	0.20	0.48

correction to y_{200} shows strong positive and negative fluctuations, that to y_{400} exhibits modest fluctuations of both signs, while the value of c determined from η decreases smoothly from 0.5, at $n_{eq}=3$, to 0.29, at $n_{eq}=9$. On the other hand, the size of the shifts in y_{200} and η correlate well and both patterns lead to the same sequence of balanced truncations. In summary, our calculated value of c is in the range $0.1<c<0.5$, in comparison to the exact value $c=8/(3\pi^2)\simeq 0.2702$.

IV. COMPARISON WITH OTHER METHODS

The SFM differs in important ways from other techniques for the high-precision calculation of critical exponents. In this section, we present brief, nontechnical comparisons between the HT, MC, FT, and SF methods.

A. High-temperature-series expansions

For the purpose of comparing results for critical exponents, we use as standards the HT-series estimates for the Ising model ($N=1$). The first row of Table VIII summarizes the results of three analyses of Nickel's 21-term series for the body-centered-cubic lattice as calculated by Zinn-Justin,[13] Chen, Fisher, and Nickel,[14] and Nickel and Rehr.[15] The quoted uncertainties denote statistical errors only, and represent ± 1, 0.675, and 1.5 standard deviations for the three respective sets of results.

The above series analyses took into consideration the first correction-to-scaling term albeit in different ways. The task of finding both the leading exponent and the first correction exponent involves an intrinsically unstable fitting procedure.[16] New techniques[10] have been developed to deal with this difficulty, e.g., Roskie's method,[12,32] a refined ratio method,[13] and a partial-differential-approximant method.[14,15] The exponent results obtained by these procedures are more or less biased. In Roskie's method, a fixed value of Δ_{400} is assigned.[32] In the ordinary differential-approximant method, an assigned Δ_{400} is varied and best values for the critical exponents determined by the Δ_{400} that yields the most universal value of γ when results are compared from certain sets of models. The exponent estimates by the partial-differential-approximant method[14] are largely unbiased, although the multicritical point is constrained and approximants used in the data analysis are selected by the criterion of their invariance under Euler transformation. For further details and comments, see Refs. 14 and 16. Since series for *different* models are extrapolated to a common universal limit (see, e.g., Figs. 7 and 8 of Ref. 16), one is confident that the HT exponents in Table VIII characterize the asymptotic behavior rather than a spurious "plateau." (The latter had been the case with earlier analysis of single series of 15 terms or less that yielded $\nu\approx 0.638$ and $\gamma\approx 1.25$.) However, since certain higher-order correction-to-scaling and/or analytic background terms are assumed to be negligible in the HT-series analyses, the value for Δ_{400} may still have the character of an effective exponent in the sense of Riedel and Wegner.[33] In contrast, such difficulties do not arise in calculations by the SFM because there the leading *and* correction-to-scaling exponents follow without a fitting procedure by matrix diagonalization.

In comparison to the FT estimates (second row of Table VIII), the HT results indicate a slightly higher value for Δ_{400} and a slightly lower one for γ (i.e., a larger η). The new SF estimates for $N=1$ exhibited in Table IV are consistent with that conclusion, although the larger confidence limits must be noted. Rehr[34] has attempted to deduce the second correction-to-scaling exponent from HT series for the spin-$\frac{1}{2}$ Ising model. Using $\nu=0.63$, he obtained $y_{400}\approx 0.79$ or, $\Delta_{400}\approx 0.50$, and an effective ex-

TABLE VIII. Summary of current estimates for the critical exponents of the Ising model ($N=1$) by the high-temperature (HT), field-theoretic (FT), and Monte Carlo (MC) methods. Results by the scaling-field (SF) method are contained in Table V. Confidence limits are one-standard-deviation statistical errors, except Refs. 14 and 15, where the uncertainties are ± 0.675 and 1.5 standard deviations, respectively.

	ν	η	γ	Δ_{400}	Reference
HT	0.6305±0.0015	0.035±0.003	1.2385±0.0025	0.52 ±0.07	13
			1.2385±0.0015	0.54 ±0.05	14
	0.6300±0.0015	0.0359±0.0007	1.237 ±0.002	0.51 ±0.03	15
FT	0.630 ±0.0015	0.031 ±0.004	1.241 ±0.002	0.498±0.020	6
	0.630 ±0.002	0.031 ±0.011	1.241 ±0.004	0.496±0.004	7
	0.628 ±0.001	0.035 ±0.002		0.50 ±0.02	46
MC	0.629 ±0.004	0.031 ±0.005		0.63 ±0.07	17

ponent $y_{422} \approx 1.4$ or $\Delta_{422} \approx 0.90$. We note that the only calculation in three dimensions of the leading odd correction-to-scaling exponent Δ_{500} is by the SFM.

No survey of recent experimental results for the Ising exponents has been gathered. For older results, the reader is referred to the reviews in Refs. 6 and 10. Beysens[35] summarizes the experimental results for ten binary mixtures and concludes that $\nu = 0.625 \pm 0.005$, $\gamma = 1.236 \pm 0.008$, $\beta = 0.326 \pm 0.002$, and $\alpha = 0.112 \pm 0.005$, with uncertainties of one standard deviation. Pestak and Chan[36] determined the correction-to-scaling exponent Δ_{400} near the liquid-gas critical point of N_2, and obtained $\gamma = 1.233 \pm 0.01$, $\beta = 0.327 \pm 0.002$, and $\Delta_{400} = 0.51 \pm 0.03$. We are not aware of an experimental determination of the correction-to-scaling exponents Δ_{500}, although several methods, of varying degrees of feasibility, have been proposed.[27,37,38]

The question has been raised whether the HT-series-expansion method can be further extended.[16] The method proved powerful for high-precision calculations of the leading relevant exponents of the Ising model. Nickel[16] has estimated a factor of 20 in resources for an extension of the series for the Ising model from 21 to 23 terms. For isotropic and anisotropic *N-vector* models, the present-day series are too short to yield unbiased results of high accuracy, and it is presumably too difficult to generate series of sufficient length.[39]

B. Monte Carlo renormalization group

A promising new development is a recent application of the MC renormalization group to the three-dimensional Ising model by Pawley, Swendsen, Wallace, and Wilson.[17] The present calculation is for simple cubic lattices of up to $64 \times 64 \times 64$ sites in an approximation that retains seven operators, including three different four-spin products. In contrast to work in two dimensions,[40] convergence is slow and the raw data for $1/\nu$ do not reach a plateau of values for neighboring lattice sizes and blocking levels. Nevertheless, after interpolating to obtain the critical coupling constant K_c and correcting for transient and finite-size effects, the authors deduce estimates for ν and η which, although exhibiting larger statistical errors (one standard deviation), are in good agreement with the HT results. They are presented in the third row of Table VIII. However, a rather poor result for the correction-to-scaling exponent, $y_{400} = 1.0 \pm 0.1$ or $\Delta_{400} = 0.63 \pm 0.07$, seems to indicate that the method has not yet converged. From the viewpoint of the SF approach, it is not surprising that a satisfactory calculation of y_{400} requires the inclusion of additional four-spin and higher-order operators. We note that Pawley *et al.*[17] find a second positive eigenvalue, which they associate with a redundant operator. They test the correctness of the relationships (2.22) and (3.1a) between the leading odd eigenvalues and η. In contrast to the SFM, they find poor agreement. The relationship for y_{321}, Eq. (3.1b), has not been tested.

Swendsen[18] has proposed to improve upon the above calculation by including 17 operators, among them one six-spin and one eight-spin operator (i.e., the eight spins on an elementary cube), and then to optimize the RG transformation. The usefulness of the MCRG approach for general N-vector models is an open question. So far, the accuracy of results for the planar model[41] is far from that of other methods.

C. Field-theoretic perturbation expansions

The major difference between the Wilson RG approach and the FT perturbation techniques is that the former involves an infinite number of coupling constants (which are called scaling fields), while the latter concentrates on the coupling constant u of the σ^4 term in the Landau Hamiltonian. The definition of the renormalization function $Z(u)$ involves perturbation theory in an essential way. The expansions are asymptotic and exact calculations can be performed only in the limit of small ϵ.[42] There are two main difficulties for the FT approach to critical phenomena in three-dimensional systems:

(i) Even once the $Z(u)$ functions are defined perturbatively, sophisticated resummation and extrapolation procedures are required for reconstructing their forms from the expansions. The available information consists of the six leading terms for $Z_\gamma(u)$, $Z_\gamma(u)$, and $Z_\beta(u)/u$ plus the behavior at large order.[6,7,10]

(ii) New functions $Z(u)$ must be determined and subsequently analyzed in order to determine higher-order corrections to scaling—a procedure that has yet to be applied in practice.

The FT estimates for the exponents of the isotropic N-vector model are widely regarded as the definitive results for three-dimensional critical phenomena. We do not discuss here whether this is justified, but instead compare in Table VIII the FT results for $N = 1$ with the corresponding results from HT, MC, and SF methods (see also the discussion in subsections A and D) and propose a series of challenges for the FT and SF methods. First, one should test, by computing via the SFM the fixed-point value of the renormalization coupling constant u^*, the FT assumption that the function $Z(u)$ is smooth and can be extrapolated to a region not accessible by direct calculation. Rehr[34] and Nickel and Sharpe[43] have computed u^* using HT series for the Ising model and find 0.1602 and 0.1594, respectively, which are to be contrasted with the FT estimate of 0.1616.[6,7] Second, the universal amplitude ratios for the isotropic N-vector model should be calculated using the SFM and compared with the FT estimates.[44] Third, it would be interesting to test the degree to which the FT estimates for the critical exponents are universal under variation of a redundant parameter, such as the normalization parameter A of Eq. (2.10). We suggest that a loss of universality in calculations involving truncations [in FT, that of the series for $Z(u)$] is one unconsidered source of systematic error.[45] Finally, we suggest that the next-to-leading critical exponents be calculated using FT methods. This involves a matrix diagonalization; therefore, in certain approximations, one may encounter (as in the SFM) the artifact of complex pairs of eigenvalues.

It is unlikely that the FT work for the isotropic N-vector model can be extended to higher order. Technical difficulties in computing large-dimensional integrals appear prohibitive. Recently, FT loop approximations using

ϵ expansion have been carried to order ϵ^5 and yielded high-precision results for the exponents ν, η, and Δ_{400} of the three-dimensional isotropic N-vector model with $N=1$, 2, and 3.[46] The results for $N=1$ are included in the second row of Table VIII. In the study of anisotropic N-vector models, FT loop expansions at fixed dimension have been employed.[47] Results for the percolation problem via the $Q=1$ Potts model are not satisfactory (for further details, see Sec. III C of Ref. 4).

D. Scaling-field method

The SFM differs from the other techniques in several ways. It is based on an exact RG equation, is nonperturbative, and yields unbiased results. It applies with only minor changes to isotropic and anisotropic N-vector models. It allows the investigation of trends in critical phenomena as functions of dimension d and number of spin components N. Finally, it is feasible to proceed to the next levels of successive approximation.

The accuracy of the exponent estimates in Table IV for the isotropic N-vector model is excellent in view of the modest length of the truncations considered. The uncertainties denote confidence limits including systematic errors. The estimates for ν, η, and Δ_{400}, although less precise, agree well with the FT results for $N=0$, 1, 2, and 3. As discussed in subsection A, for $N=1$, they are consistent with the conclusion from HT series of higher values of Δ_{400} and η than the FT estimates. If we assume that this trend is also significant for $N\neq 1$, we can make the following statements. For η and Δ_{400}, the SF estimates indicate slightly higher values than the FT results also for the other values of N. For ν, the SF estimates are lower, at $N=0$ and 1, and higher, at $N=2$ and 3, than the FT results. We note that for $N=2$ this conclusion would be consistent with the experimental result at the λ transition in ^{4}He, where $\nu\approx 0.6717\pm 0.0004$ with an uncertainty of one standard deviation excluding systematic errors.[48] Furthermore, we have obtained new information about the spectrum of correction-to-scaling exponents.

We believe that the SFM provides a method of successive approximation for solving the Wilson equation. There is no proof that convergence must occur. However, general observations indicate that high-precision results for leading critical behavior can be achieved keeping only certain kinds and limited numbers of operators in the expansion of the Landau Hamiltonian. Although approximation takes place by the severe device of truncation, it is controlled by the "principle of balance" and the order in which successive truncations are constructed is fine-tuned by feedback from the fixed point under consideration. The idea of a "marker" is used to stop the sequence of truncations before it enters the "noisy" regime. We believe that the procedure of approximation does not bias the results for critical exponents. The length of the sequence of truncations is optimized (or, the effect of unavailable terms in the Landau Hamiltonian is minimized) by the choice of the redundant normalization parameter A. Varying a redundant parameter is also an important device to test universality or the degree of convergence of the results. The only other method that examined the effect of a "tweaking" parameter was the HT technique. Presumably, our optimization procedure can be improved. A severe test of the SFM will occur at the next level of approximation, when scaling fields of the type $\mu_{\overline{mpt}}$ with $p=4$ will be included, and μ_{261} will act as the "marker." One current problem that can lead to systematic errors for the leading irrelevant eigenvalues is their tendency to form complex pairs. Our proposal is that, as the number of equations $n_{\rm eq}$ is increased, the effect of truncation will be further removed to lower-lying eigenvalues, resulting in a further settling of the fluctuations in the values of the exponents as functions of $n_{\rm eq}$ (as exhibited in Figs. 7—10). Hopefully, then, any problems with formation of complex pairs of eigenvalues will also be removed to lower levels.

The scope of the SFM is discussed in Secs. I and V of Ref. 1. Here we have demonstrated that high precision can be achieved in the SF calculation of critical exponents. The determination, e.g., of scaling functions, critical amplitudes, or the fixed-point value of the renormalized coupling constant u^*, has yet to be addressed. Several crossover phenomena have been investigated for various cubic and Potts models, but so far only for short truncations.[3,4] In these studies, as well as the ones of the irrelevant eigenvalues of the isotropic N-vector model (see Sec. III B), it proved useful that trends in critical behavior could be followed as functions of d and N. We expect that this idea can be applied advantageously to a wide variety of problems. For example, for the Potts model, the interpolation as a function of spatial dimension d between the upper and lower critical dimensionalities led to a better understanding of the role of critical and tricritical fixed points.[4] The versatility of the SF approach derives from the fact that the exact Wilson equation is an equation for Landau RG Hamiltonians. The SF coupling coefficients can be calculated for the dimension of interest, including noninteger dimensions.[3] And, as described in Sec. II C *4*, there are no technical reasons that would force one to stop the calculation at the present level of approximation.

V. SUMMARY

A method for the solution by successive approximation of Wilson's exact RG equation for critical phenomena has been proposed. The approach is termed scaling-field method (SFM). In this paper we have demonstrated that the method is well suited for the high-precision calculation of critical exponents. In this and other papers[1,3–5] the method has been shown to offer a versatile and reliable tool for the investigation of critical phenomena in spin systems over a large range of dimensions. The approach is not limited to the level of approximation discussed here. A discussion of the steps necessary to extend our calculation has been included in Sec. II.

It is concluded that the SF approach to the Wilson equation offers a sound basis for a large-scale computing effort of the critical parameters for isotropic and anisotropic N-component spin models. We believe that the method has the potential for surpassing the field-theoretic approach as the best source of RG data for such systems.

ACKNOWLEDGMENTS

This research was performed at the University of Washington and was supported in part by the National Science Foundation under Grants No. DMR-79-20785 and No. DMR-83-19301. One of us (E.K.R.) is grateful for the hospitality extended to him by Professor J. Villain at the Centre d'Etudes Nucléaires, Grenoble, France, where part of this manuscript was prepared. The authors acknowledge with thanks the hospitality of the Departments of Physics at the University of Notre Dame (E.K.R.) and the University of Washington (K.E.N.). Discussions with Professor E. Domany and Professor J. J. Rehr and the continued encouragement of Professor J. D. Dow are also gratefully acknowledged.

APPENDIX A: PARAMETRIZATION OF THE LANDAU HAMILTONIAN

Three parametrizations of the Landau Hamiltonian (2.2) are used: Either Eqs. (2.2) or (2.4), or

$$H_l[\sigma]=H_G^*[\sigma]+\sum_{\bar{m}\ \text{even}}\int_{\underset{\sim}{q}_1,\ldots,\underset{\sim}{q}_{\bar{m}}}\prod_{i=1}^{\bar{m}}\psi(q_i)v_{\bar{m}}(\underset{\sim}{q}_1,\ldots,\underset{\sim}{q}_{\bar{m}};l)[\vec{\sigma}(q_1)\cdot\vec{\sigma}(q_2)]\cdots[\vec{\sigma}(q_{\bar{m}-1})\cdot\vec{\sigma}(q_{\bar{m}})]\delta(\underset{\sim}{q}_1+\cdots+\underset{\sim}{q}_{\bar{m}})\ . \tag{A1}$$

Equation (A1) defines a new set of functions $v_{\bar{m}}\{\underset{\sim}{q}_i;l\}$ that are related to the functions $u_{\bar{m}}\{\underset{\sim}{q}_i;l\}$ of Eq. (2.2). The $v_{\bar{m}}\{\underset{\sim}{q}_i;l\}$ functions are found through expansion of the Gaussian eigenfunctionals [Eqs. (2.12)–(2.14)]. The isotropic homogeneous functions $f_{\bar{m}pt}\{\underset{\sim}{q}_i\}$ defined in Eq. (2.15) allow expansions of both the $u_{\bar{m}}\{\underset{\sim}{q}_i;l\}$ and $v_{\bar{m}}\{\underset{\sim}{q}_i;l\}$ functions,

$$v_{\bar{m}}(\underset{\sim}{q}_1,\ldots,\underset{\sim}{q}_{\bar{m}};l)=\sum_{p,t}v_{\bar{m}pt}(l)f_{\bar{m}pt}(\underset{\sim}{q}_1,\ldots,\underset{\sim}{q}_{\bar{m}})\ , \tag{A2}$$

etc. Then, for the truncations studied here,

$$v_{\bar{m}00}(l)=\frac{1}{\bar{m}!}\left[\mu_{\bar{m}00}(l)+\sum_{\substack{\bar{k}>\bar{m},\\ \bar{k}\ \text{even}}}C(\hat{k},\hat{k}-\hat{m})R_0^{\hat{k}-\hat{m}-1}\times\left\{R_0\mu_{\bar{k}00}(l)+\left[\frac{\bar{k}-\bar{m}}{\bar{k}}\right]R_2\left[\mu_{\bar{k}21}(l)-\left[\frac{N}{N+\bar{k}-2}\right]\mu_{\bar{k}22}(l)\right]\right\}\right]\ . \tag{A3}$$

$$v_{221}(l)=\frac{1}{2}\left[\mu_{221}(l)+\sum_{\substack{\bar{k}>2,\\ \bar{k}\ \text{even}}}C(\hat{k},\hat{k}-1)\left[\frac{2}{\bar{k}}\right]R_0^{\hat{k}-1}\left[\mu_{\bar{k}21}(l)-\left[\frac{N}{N+\bar{k}-2}\right]\mu_{\bar{k}22}(l)\right]\right]\ , \tag{A4}$$

$$v_{241}(l)=\tfrac{1}{2}\mu_{241}(l)\ , \tag{A5}$$

and, for $\bar{m}>2$ and even,

$$v_{\bar{m}21}(l)=\frac{1}{\bar{m}!}\left[\mu_{\bar{m}21}(l)+\sum_{\substack{\bar{k}>\bar{m},\\ \bar{k}\ \text{even}}}C(\hat{k},\hat{k}-\hat{m})\left[\frac{\bar{m}}{\bar{k}}\right]R_0^{\hat{k}-\hat{m}}\mu_{\bar{k}21}(l)\right]\ , \tag{A6}$$

$$v_{\bar{m}22}(l)=\frac{1}{\bar{m}!}\left[\mu_{\bar{m}22}(l)+\sum_{\substack{\bar{k}>\bar{m},\\ \bar{k}\ \text{even}}}C(\hat{k},\hat{k}-\hat{m})\left[\frac{\bar{m}(N+\bar{m}-2)}{\bar{k}(N+\bar{k}-2)}\right]R_0^{\hat{k}-\hat{m}}\mu_{\bar{k}22}(l)\right]\ , \tag{A7}$$

where $\hat{m}=\bar{m}/2$, etc., and

$$C(\hat{m},\hat{i})=\frac{(-1)^{\hat{i}}}{\hat{i}!}\prod_{i=1}^{\hat{i}}\frac{N+2(\hat{m}-i)}{2(\hat{m}-i)+1}\ . \tag{A8}$$

The integral R_p is

$$R_p=\tfrac{1}{2}\int_{\underset{\sim}{q}}q^pg(q)\ , \tag{A9}$$

where

$$g(q)=\frac{\psi^2(q)}{u_G^*(q)}=\frac{\exp(-2q^2)}{Aq^2[Aq^2+\exp(-2q^2)]}\ . \tag{A10}$$

The coefficients $v_{\bar{m}pt}\{\underset{\sim}{q}_i;l\}$ are related to the $u_{\bar{m}pt}\{\underset{\sim}{q}_i;l\}$ through a small-q expansion of $g(q)$,

$$u_{\bar{m}00}(l)=v_{\bar{m}00}(l)\ , \tag{A11}$$

$$u_{221}(l)=\frac{A}{2}+2(1-A)v_{200}(l)+v_{221}(l)\ , \tag{A12}$$

$$u_{241}(l)=\frac{A(2-A)}{2}+(3A^2-8A+2)v_{200}(l)$$
$$+2(1-A)v_{221}(l)+v_{241}(l)\ , \tag{A13}$$

and, for $\bar{m}>2$,

$$u_{\bar{m}21}(l)=v_{\bar{m}21}(l)+2\bar{m}(1-A)v_{\bar{m}00}(l) \tag{A14}$$

and

$$u_{\bar{m}22}(l)=v_{\bar{m}22}(l)\ . \tag{A15}$$

APPENDIX B: $N=-2$, OR THE GAUSSIAN MODEL

The exponents of the isotropic N-vector model in the limit $N=-2$ are the Gaussian critical ones.[49] Here we discuss the distinction between the Gaussian *critical* and the Gaussian *tricritical* fixed points at $N=-2$, as well as show explicitly the behavior of the line of fixed points for both of these Gaussian solutions.

In the SF approach, the limit $N=-2$ is special because, for this N value, the SF equations decouple into two sets. For all truncations considered in this paper, the "Gaussian" set that decouples from the rest is Trun(1,1,1,1). We conjecture that the decoupling of the equations into a "Gaussian" set $\{\mu_{m'}\}$ and a remainder set $\{\mu_{m''}\}$ is exact, i.e., that

$$\frac{d\mu_{m'}}{dl}=G_{m'}\{\mu_{m'}\}\ , \tag{B1}$$

$$\frac{d\mu_{m''}}{dl}=F_{m''}\{\mu_{m'},\mu_{m''}\}\ . \tag{B2}$$

The decoupling implied by Eqs. (B1) and (B2) occurs because

$$a_{m'j''k}\propto(N+2) \tag{B3}$$

for $\mu_{m'}\in\{\mu_{m'}\}$ and $\mu_{j''}\in\{\mu_{m''}\}$. The set $\{\mu_{m'}\}$ is probably composed solely of μ_{2pt} for all p,t and μ_{4pt} for $p\neq0$ and $t\neq1$; however, we were not able to show this in general.[50]

The decoupling of the SF equations at $N=-2$ leads to a Gaussian critical fixed-point solution:

$$\mu^*_{m'}=0,\ \ \mu^*_{m''}\neq0\ ,$$
$$y^c_{m'}=y^G_{m'},\ \ y^c_{m''}<0,\ \ \Delta^*=\eta^c=0\ , \tag{B4}$$

in addition to the usual Gaussian tricritical solution:

$$\mu^*_m=0\ \text{ for all } m\ ,$$
$$y^t_m=y^G_m,\ \ \Delta^*=\eta^t=0\ . \tag{B5}$$

The distinction between these two solutions is that $\mu^*_{400}=0$ for the Gaussian tricritical one, and thus $y^t_{400}=1$, while $\mu^*_{400,c}\neq0$ for the Gaussian critical one, and thus $y^c_{400}<0$. Equation (B2) must be solved numerically for the SF coordinates $\mu^*_{m''}$ and the eigenvalues $y^c_{m''}$. The latter are found to be noninteger.

Finally, both for the Gaussian critical and the usual Gaussian tricritical fixed points, the line of fixed points as function of μ^*_{221} may be studied. One may trivially derive the required coupling coefficients a_{mjk} from Eqs. (4.3) and (4.9) of I:

$$-2(1+2q^2+\Delta)\psi^2(q)q^{p_j+p_k}=\sum_{p_m}a_{2p_m1;2p_j1;2p_k1}q^{p_m}\ , \tag{B6}$$

from which one finds (for $\Delta=0$)

$$\frac{d\mu_{200}}{dl}=2\mu_{200}-2\mu^2_{200}\ , \tag{B7}$$

$$\frac{d\mu_{221}}{dl}=-4(2-A)\mu^2_{200}-4\mu_{200}\mu_{221}\ , \tag{B8}$$

$$\frac{d\mu_{241}}{dl}=-2\mu_{241}-2(3A^2-12A+6)\mu^2_{200}$$
$$-8(2-A)\mu_{200}\mu_{221}-2\mu^2_{221}-2\mu_{200}\mu_{241}\ , \tag{B9}$$

etc. Equations (B7)—(B9) have the simple solution given by Eqs. (2.26) and

$$\Delta^*=0,\ \ y_{2p1}=y^G_{2p1}=2-p\ , \tag{B10}$$

which is described in Sec. II B. Hence, for $\Delta^*=0$, there exists a line of Gaussian fixed-point solutions as functions of μ^*_{221} or normalization of the spins σ and momentum q. If a nonzero Δ is chosen, then only *one* fixed-point solution, with $y_{200}=2$, is found with a corresponding eigenvalue y_{221} given by

$$y_{221}=-2\Delta\ . \tag{B11}$$

Thus the line of Gaussian fixed points is destroyed by the wrong choice of Δ.

[1]E. K. Riedel, G. R. Golner, and K. E. Newman, Ann. Phys. (N.Y.) (to be published), which is referred to as I in the present paper.

[2]K. G. Wilson and J. Kogut, Phys. Rep. **12C**, 75 (1974), especially Sec. 11 and Appendix A. We refer to Eq. (11.17) of this work as the Wilson equation. This equation was first reported by Wilson at the Irvine Conference, 1970 (unpublished).

[3]K. E. Newman and E. K. Riedel, Phys. Rev. B **25**, 264 (1982); **30**, 2924(E) (1984).

[4]K. E. Newman, E. K. Riedel, and S. Muto, Phys. Rev. B **29**, 302 (1984); **30**, 2924(E) (1984).

[5]Preliminary results can be found in E. K. Riedel and K. E. Newman, in *Statics and Dynamics of Nonlinear Systems*, edited by G. Benedek, H. Bilz, and R. Zeyer (Springer, Berlin, 1983), p. 80. See also K. E. Newman and E. K. Riedel, Bull. Am. Phys. Soc. **29**, 396 (1984).

[6]J. C. LeGuillou and J. Zinn-Justin, Phys. Rev. B **21**, 3976 (1980).

[7]G. A. Baker, Jr., B. G. Nickel, and D. I. Meiron, Phys. Rev. B **17**, 1365 (1978).
[8]F. J. Wegner, Phys. Rev. B **5**, 4529 (1972).
[9]B. G. Nickel, D. I. Meiron, and G. A. Baker, Jr., University of Guelph Report, 1977 (unpublished).
[10]For reviews, see *Phase Transitions (Cargèse, 1980)*, edited by M. Lévy, J. C. LeGuillou, and J. Zinn-Justin (Plenum, New York, 1982).
[11]B. G. Nickel, Physica **106A**, 48 (1981).
[12]R. Z. Roskies, Phys. Rev. B **24**, 5305 (1981).
[13]J. Zinn-Justin, J. Phys. (Paris) **42**, 783 (1981).
[14]J. H. Chen, M. E. Fisher, and B. G. Nickel, Phys. Rev. Lett. **48**, 630 (1982).
[15]B. G. Nickel and J. J. Rehr (unpublished).
[16]B. G. Nickel, in *Phase Transitions (Cargèse, 1980)*, Ref. 10, p. 291.
[17]G. S. Pawley, R. H. Swendsen, D. J. Wallace, and K. G. Wilson, Phys. Rev. B **29**, 4030 (1984).
[18]R. H. Swendsen, Phys. Rev. Lett. **52**, 2321 (1984).
[19]R. B. Pearson, D. Toussaint, and J. L. Richardson, J. Comput. Phys. **51**, 241 (1983).
[20]Our notation Δ_m is defined in Sec. II A by Eq. (2.20). Different notations are in use for the leading correction-to-scaling exponent, e.g., Δ_1, θ, and $\omega\nu$, which denote the same quantity as our Δ_{400}.
[21]G. R. Golner and E. K. Riedel, Phys. Rev. Lett. **34**, 171 (1975); Phys. Lett. **58A**, 11 (1976).
[22]See also F. J. Wegner, in *Phase Transitions and Critical Phenomena*, edited by C. Domb and M. S. Green (Academic, London, 1976), Vol. 6, p. 7.
[23]T. L. Bell and K. G. Wilson, Phys. Rev. B **10**, 3935 (1974).
[24]F. J. Wegner, J. Phys. C **7**, 2098 (1974).
[25]T. L. Bell and K. G. Wilson, Phys. Rev. B **11**, 3431 (1975).
[26]See for example, F. B. Hildebrand, *Introduction to Numerical Analysis* (McGraw-Hill, New York, 1974). Considerable care must be applied in choosing input for the Newton-method routine since failure to find a fixed point might lead one to incorrectly identify a truncation as unbalanced. When a guess from a previous truncation is not sufficient for Newton's method to converge, the fixed-point condition for the new scaling field μ_j is relaxed to $d\mu_j/dl \neq 0$ and μ_j is incremented successively so that $|d\mu_j/dl|$ decreases, while still requiring all other derivatives $d\mu_m/dl$ to vanish.
[27]J. F. Nicoll and R. K. P. Zia, Phys. Rev. B **23**, 6157 (1981).
[28]J. F. Nicoll, Phys. Rev. A **24**, 2203 (1981).
[29]The situation is analogous to the consistency test provided by a set of the correction-to-scaling exponents of the decoupled Ising fixed point. For details see Ref. 3.
[30]F. C. Zhang and R. K. P. Zia, J. Phys. A **15**, 3303 (1982).
[31]See, for example, S.-k. Ma, *Modern Theory of Critical Phenomena* (Benjamin, Reading, Mass., 1976), Chap. X.
[32]Results by B. G. Nickel and M. Dixon [Phys. Rev. B **26**, 3965 (1982)] using $\Delta_1 = 0.5$ are $\nu = 0.630 \pm 0.003$, $\gamma = 1.237 \pm 0.003$, and $\eta = 2 - \gamma/\nu = 0.036 \pm 0.002$. See also J. Adler, M. Moshe, and V. Privman [Phys. Rev. B **26**, 1411 (1982)] and J. Adler [J. Phys. A **16**, 3585 (1983)].
[33]E. K. Riedel and F. J. Wegner, Phys. Rev. B **9**, 294 (1974).
[34]J. J. Rehr, J. Phys. A **12**, L179 (1979).
[35]D. Beysens, in *Phase Transitions (Cargèse, 1980)*, Ref. 10, p. 25.
[36]M. W. Pestak and M. H. W. Chan, Phys. Rev. B **30**, 274 (1984).
[37]M. R. Moldover and R. W. Gammon, J. Chem. Phys. **80**, 528 (1984); M. W. Pestak and M. H. W. Chan, Bull. Am. Phys. Soc. **29**, 227 (1984).
[38]M. P. A. Fisher and M. Wortis, Phys. Rev. B **29**, 6252 (1984). These authors show that the leading curvature correction δ of a large spherical drop should be controlled either by $|t|^{\Delta_{321}-\nu}$ (where $\Delta_{321} = 1-\alpha-\beta$) or by $|t|^{\Delta_{500}-\nu}$, with the type of dependence on the temperature t being determined by the value of Δ_{500} for three dimensions. Using results given here, we find that the leading temperature dependence of δ is $|t|^{\Delta_{321}-\nu}$, i.e., δ is only weakly divergent as a function of t.
[39]M. E. Fisher and J. H. Chen, in *Phase Transitions (Cargèse, 1980)*, Ref. 10, p. 169.
[40]R. H. Swendsen, in *Real-Space Renormalization*, edited by T. W. Burkhardt and J. M. J. van Leeuwen (Springer, New York, 1982), p. 57.
[41]R. H. Swendsen, Phys. Rev. B **27**, 391 (1983).
[42]D. J. Amit, *Field Theory, the Renormalization Group, and Critical Phenomena* (McGraw-Hill, New York, 1978).
[43]B. G. Nickel and B. Sharpe, J. Phys. A **12**, 1819 (1979).
[44]C. Bervillier and C. Godrèche, Phys. Rev. B **21**, 5427 (1980); C. Bagnuls and C. Bervillier, *ibid.* **24**, 1226 (1981).
[45]Part of the systematic error in the FT results for the critical exponents can be estimated by comparing different methods of analysis of the expansion of $Z[u]$ functions. For example, D. Z. Albert [Phys. Rev. B **25**, 4819 (1982)] has used a different coupling-constant transformation before Borel resummation and obtained results that differ slightly from those of Refs. 6 and 7.
[46]S. G. Gorishny, S. A. Larin, and F. V. Tkachov, Phys. Lett. **101A**, 120 (1984).
[47]J. S. Reeve, J. Phys. A **15**, L521 (1982).
[48]A. Singsaas and G. Ahlers (unpublished). See also G. Ahlers, in *Phase Transitions (Cargèse, 1980)*, Ref. 10, p. 1.
[49]R. Balian and G. Toulouse, Phys. Rev. Lett. **30**, 544 (1973).
[50]To understand why μ_{400} and μ_{4p1} are *not* included in the set $\{\mu_{m'}\}$, consider the dependence of the Gaussian component of the Landau Hamiltonian (2.2), i.e., the function $u_2(q;l)$, on the set of scaling fields $\mu_{\overline{mpt}}$. Definitions (A1) and (A2) relate this function to $v_{200}(l)$, for example, and thus also to the infinite set of scaling fields μ_m. From Eq. (A3) we find that, for $N=-2$, there will be no contributions to $u_2(q;l)$ from the scaling fields μ_{400} and μ_{4p1}, whereas there will, in general, be contributions from all other scaling fields μ_{4pt}.